5-2016

DEVELOPMENT OF A DATABASE FOR RAPID APPROXIMATION OF SPACECRAFT RADIATION DOSE DURING JUPITER FLYBY

Sarah Gilbert Stewart
University of Tennessee - Knoxville, sgilber4@vols.utk.edu

To the Graduate Council:

I am submitting herewith a thesis written by Sarah Gilbert Stewart entitled "DEVELOPMENT OF A DATABASE FOR RAPID APPROXIMATION OF SPACECRAFT RADIATION DOSE DURING JUPITER FLYBY." I have examined the final electronic copy of this thesis for form and content and recommend that it be accepted in partial fulfillment of the requirements for the degree of Master of Science, with a major in Aerospace Engineering.

James E. Lyne, Major Professor

We have read this thesis and recommend its acceptance:

Lawrence W. Townsend, Zhili Zhang

Accepted for the Council:
Carolyn R. Hodges

Vice Provost and Dean of the Graduate School

(Original signatures are on file with official student records.)

DEVELOPMENT OF A DATABASE FOR RAPID APPROXIMATION OF SPACECRAFT RADIATION DOSE DURING JUPITER FLYBY

A Thesis Presented for the
Master of Science
Degree
The University of Tennessee, Knoxville

Sarah Gilbert Stewart
May 2016

ACKNOWLEDGEMENTS

First, I would like to convey my deepest appreciation to my advisor, Dr. Evans Lyne, for his excellent guidance, patience and encouragement. This thesis would not have been possible without his support. I would also like to thank my other committee members, Dr. Lawrence Townsend and Dr. Zhili Zhang, for their counsel and guidance. Special thanks goes to fellow graduate student, Jakob Brisby, for his knowledge and assistance with the computer science aspect of my project.

I would like to express my sincere gratitude to my family. First, I would like to thank my parents, Dan and Betsy Gilbert, who have spent countless hours supporting me throughout my time at graduate school. My dream to earn a Master's Degree would not have been possible without their emotional, financial and spiritual support. I would like to thank my sister, Leah Hughes, and brother, Adam Gilbert, for their many trips to visit me in Knoxville and immeasurable amount of encouraging phone calls and text messages. I would like to thank my son, Levi, for the daily joyfulness he has brought into my life. Finally, I would like to thank my husband, Brian Stewart, for being my greatest supporter throughout the last three years. Without him, I would not have been able to achieve this goal. Huge thanks, love and appreciation go to him for managing our long-distance marriage with grace and generosity.

ABSTRACT

Interplanetary and deep space missions greatly benefit from the utilization of gravitational assists to reach their final destinations. By closely "swinging by" a planet, a spacecraft can gain or lose velocity or change directions without requiring any expenditure of propulsion. In today's budget-driven design environment, gravity assist flybys reduce the need for on-board fuel and propulsion systems, thereby reducing overall cost, increasing payload and mission capacity, increasing mission life, and decreasing travel time. It is expected that many future missions will also be designed to swing by Jupiter in order to utilize a gravity assist. However, there is a risk associated with choosing to flyby Jupiter: increased exposure to radiation. Exposure to radiation can severely impact spacecraft electronic systems. Since today's spacecraft consist of sophisticated circuits that operate at low voltages and currents, the effects of radiation have become increasingly important. Harsh radiation environments can have damaging effects on spacecraft electronics that may ultimately lead to mission failure. Historically, analysts use trapped particle environment data recorded from previous missions in conjunction with the planned trajectory of their individual mission to predict radiation exposure at Jupiter. Until now, no database existed that lists potential radiation exposure for a variety of possible Jupiter flyby trajectories. This thesis and associated tools allow radiation dose to be more easily determined during preliminary mission planning. Over 16,000 potential Jupiter flyby trajectories were generated via the Program to Optimize Simulated Trajectories (POST). These trajectories were then input into the European Space Agency's (ESA) Space Environment Information System (SPENVIS) to predict the total radiation dose behind 3 mm of Aluminum shielding. SPENVIS is web-based software that has stored trapped particle models for Jupiter. Once run through SPENVIS, total flyby radiation dosage was stored for each trajectory, and an algorithm was developed that allows for interpolation and approximation of dose for cases not in the original database. This algorithm should be useful to future space mission designers who are

looking to utilize a gravity assist at Jupiter and will allow a quick comparison of multiple mission scenarios with respect to flyby radiation dose.

TABLE OF CONTENTS

LIST OF TABLES

LIST OF FIGURES

CHAPTER I
INTRODUCTION AND GENERAL INFORMATION

Background

Interplanetary and deep space missions greatly benefit from the utilization of gravitational assists to reach their final destinations. By closely "swinging by" a planet, a spacecraft can gain or lose velocity or change directions without requiring any propulsion. In today's budget-driven design environment, gravity assist flybys reduce the need for on-board fuel and propulsion systems, thereby reducing overall cost, increasing payload and mission capacity, and decreasing travel time. The most recent mission to utilize this benefit was NASA's New Horizons spacecraft. While en route to Pluto, New Horizons received a gravity assist during a flyby encounter with Jupiter. The assist shortened travel time to Pluto by 3 years. [1]

It is expected that many future missions will also be designed to swing by Jupiter in order to utilize a gravity assist. There is a risk associated with choosing to fly by Jupiter: increased exposure to radiation. Due to many factors, Jupiter has the most intense radiation environment in our solar system.

Exposure to radiation can severely impact spacecraft electronic systems. Since today's spacecraft consist of sophisticated circuits that operate at low voltages and currents, the effects of radiation have become increasingly important. Modern electronics feature advanced architectures that include smaller components, more intricate and multifaceted structures, and the use of heavy metals, all of which make today's modern electronics more vulnerable to radiation-induced failures than previous systems. [2] Harsh radiation environments can have damaging effects on spacecraft electronics that may ultimately lead to mission failure.

Historically, analysts have used trapped particle environment data recorded from previous missions in conjunction with the planned trajectory of their individual mission to predict radiation exposure at Jupiter. There is no database that lists potential radiation exposure for a variety of possible Jupiter flyby trajectories.

Are there optimized flyby trajectories that expose spacecraft to minimal radiation dosages? What are these flybys a function of? Are there flyby trajectories that have an extraordinary risk of radiation exposure? What trajectory provides the best gravitational assist with the lowest radiation exposure for a given mission? These are the types of questions that I hope can be addressed with a database for rapid approximations of radiation exposure during Jupiter flyby.

Objectives

Currently, there is a disjointed process for finding radiation dosage for Jupiter flybys. Mission planners must use many different codes and tools to find an estimated dosage for their desired flyby parameters. Preliminary mission planning would benefit from an approximation tool. The objective of this thesis is to develop such a tool, a quick and simple way to approximate radiation dosages. The idea was to enable mission planners to compare dosages for a plethora of flyby trajectories, rather than having to go through the detailed process for each trajectory considered.

CHAPTER II
LITERATURE REVIEW

Gravity Assist Maneuvers

As previously mentioned, there are many benefits of utilizing a gravity assist maneuver. Gravity assists reduce the need for on-board fuel and propulsion systems, thereby reducing overall cost, increasing payload and mission capacity, and decreasing travel time to final destinations. Gravity assists are accomplished by efficiently using the energy that can be obtained by a space vehicle during a planetary encounter. For a passing vehicle, the planet appears as a field of force moving relative to the heliocentric coordinate system. This means work will be done on the spacecraft. Depending on the geometry of the flyby, the spacecraft can experience either an increase or decrease in its heliocentric energy. [3]

Early Work and Discovery

During early space missions, gravity assist techniques did not exist. However, in 1961, a 25-year-old mathematics graduate named Michael Minovitch decided to take on the hardest problem in orbital mechanics: the three-body problem. The three bodies refer to the sun, a planet and a third object. The problem was predicting how the Sun and planet would influence the third object's trajectory. Astronomers had been studying the three-body problem for over 300 years to no avail. In 1961, the fastest computer on Earth was IBM's 7090. Using this computer, Minovitch coded a set of equations to apply to the problem. During an internship at NASA's Jet Propulsion Laboratory (JPL), he fed data on planetary orbits into his model and achieved an extraordinary breakthrough. Minovitch had shown that as a spacecraft flew close to a planet that orbited the sun, that spacecraft could be accelerated away from the sun without the use of a

propulsion system. However, with the distraction of Project Apollo, no one at NASA noticed Minovitch's breakthrough. [4]

Later, in 1964, another JPL intern named Gary Flandro began to look at whether the solution to the three-body problem could be put to practical use in exploring the outer planets. [4] He discovered a rare geometric alignment of the outer planets that occurs every 176 years. He conceived the "grand tour" multi-planet mission utilizing a gravity assist technique that would reduce flight duration from 40 years down to less than ten years. His work led to the success of the Voyager missions. Later, in 1965, Flandro studied gravity assist trajectories to Pluto; these trajectories were the basis for the New Horizons mission which flew by Pluto in July 2015. [5]

Utilizing Energy Derived from the Gravitational Field of Jupiter

Gary Flandro published a paper in 1966 that outlined his methodology for a Jupiter gravity assist maneuver. [3] Figure 1 explains the flyby process. [6] The variables are defined as follows:

V_i : pre-flyby heliocentric velocity vector of the spacecraft
V_0: post-flyby heliocentric velocity vector of the spacecraft.
V_i' : pre-flyby velocity vector of the spacecraft relative to the planet
V_0' : post-flyby velocity vector of the spacecraft relative to the planet
V_p : heliocentric velocity vector of the planet (assumed constant during the flyby)

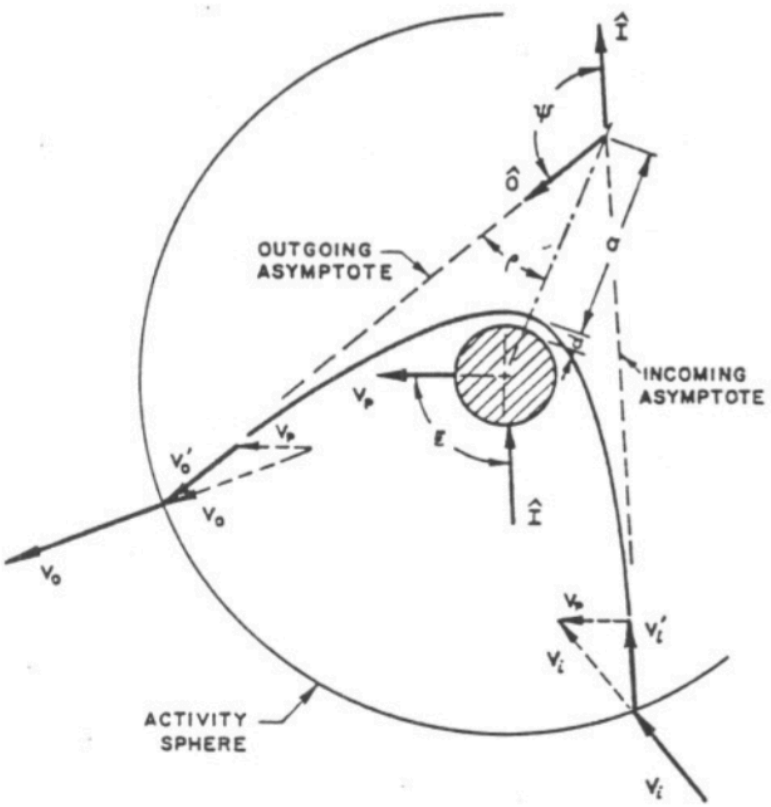

Figure 1. Flyby encounter hyperbola [3]

The heliocentric energy of the spacecraft prior to the planetary encounter is as follows:

$$E_i = \frac{V_i \cdot V_i}{2} \tag{1}$$

While the heliocentric energy after the encounter is:

$$E_0 = \frac{V_0 \cdot V_0}{2} \tag{2}$$

So the resultant change in energy is:

$$\Delta E = \frac{1}{2}[V_0 \cdot V_0 - V_i \cdot V_i] \tag{3}$$

Noting the geometric relations from Figure 1:

$$\begin{aligned} V_i' &= V_i - V_p \\ V_0' &= V_0 - V_p \end{aligned} \tag{4}$$

Assuming constant spacecraft mass and no propulsion maneuvers completed during the flyby, energy is conserved relative to the planet. This means:

$$|V_0'| = |V_i'| \equiv V_h \tag{5}$$

where V_h is the hyperbolic excess speed of the spacecraft relative to the planet. The resultant change in energy can now be written as:

$$\Delta E = V_p \cdot (V_0' - V_i') \tag{6}$$

Finally, the geometric properties of the energy equation can be clarified as follows:

$$V_p = v_p \hat{P} \tag{7}$$

$$V_i' = v_h \hat{I} \tag{8}$$

$$V_0' = v_h \hat{O} \tag{9}$$

where v_p is the speed of the planet and v_h is the hyperbolic excess speed of the spacecraft relative to the planet; $\hat{P}$, $\hat{I}$ and $\hat{O}$ are the unit vectors in the directions of the planet's velocity, incoming spacecraft velocity and outgoing spacecraft velocity, respectively. The energy equation then becomes:

$$\Delta E = v_p v_h \left[\hat{P} \cdot \left(\hat{O} - \hat{I}\right)\right] \tag{10}$$

It is convenient to write the equation in the form:

$$\Delta E = fE^* \tag{11}$$

The coefficient f is known as the energy change index and represents a number between -1 and 1 that determines the magnitude and sign of energy change achieved during the flyby. It is defined as:

$$f = \frac{\hat{P} \cdot (\hat{O} - \hat{I})}{2} \tag{12}$$

The characteristic energy, E^*, is defined as:

$$E^* = 2v_p v_h \tag{13}$$

E^* is the maximum energy increase obtainable for a given spacecraft velocity and planet. This maximum value is unobtainable because it requires a deflection angle of 180° which requires the space vehicle to travel directly through the planet. The maximum value of E^* for a given hyperbolic excess speed depends on the velocity of the chosen planet for a gravity assist. Due to Mercury's closeness to the sun and its high heliocentric velocity, a flyby of the swift planet would result in the maximum value of E^* for any given hyperbolic excess speed. This is shown in figure 2. [3]

The maximum value of the energy change index (f) depends on the ability of the selected planet to deflect the spacecraft's trajectory. The magnitude of the deflection angle (Ψ) is a function of: the gravitational constant of the planet (μ), the hyperbolic excess speed of the space vehicle, the radius of the planet (R_p) and

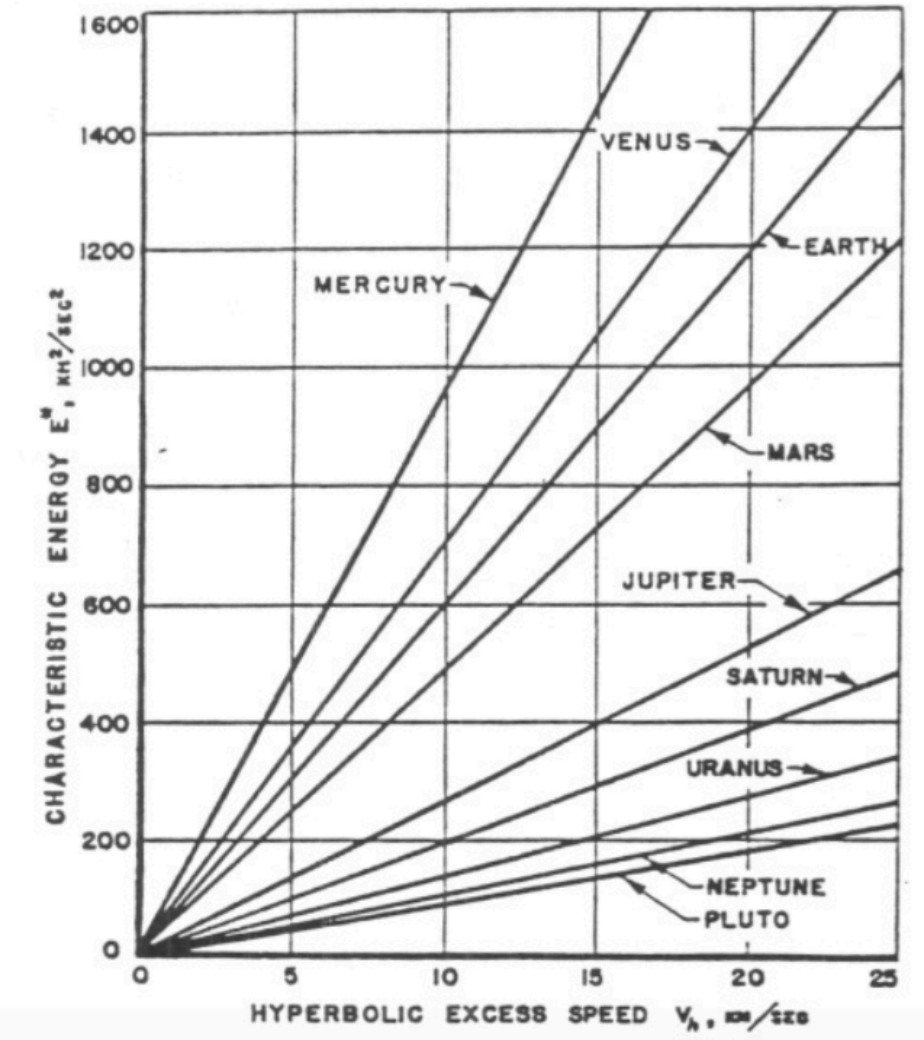

Figure 2. Characteristic energy vs. hyperbolic excess speed of spacecraft [3]

the distance of closest approach (d). It can be defined as:

$$\Psi = 2\sin^{-1}\left[1 + \frac{v_h^2}{\mu}(d + R_p)\right]^{-1} \tag{14}$$

The maximum allowable deflection angle (Ψ_{max}) occurs when the flight path just grazes the radius of the planet (R_p). In this case, R_p is equal to the equatorial radius of the planet's mantle and atmosphere in addition to a reasonable error contingency. The maximum allowable deflection angle can be written as:

$$\Psi_{max} = 2\sin^{-1}\frac{\mu}{\mu + v_h^2 R_p} \tag{15}$$

Figure 3 shows plots of Ψ_{max} versus hyperbolic excess velocity for all planets of the solar system. As expected, Jupiter is capable of the largest flight path deflection due to its large mass.

In order to assess the abilities of planets to influence the trajectories of spacecraft, one must compare the maximum change in energy versus hyperbolic excess speed for each planet. This is shown in Figure 4. One might assume that Jupiter is capable of producing the largest energy change simply due to its size. However, that is not the case. As seen in the chart, for low hyperbolic excess speeds (v_h< 10 km/sec) the smaller and faster inner planets can produce larger changes in energy. This is due to the high heliocentric speed of the planets that are closest to the Sun. At higher hyperbolic excess speeds, massive planets are able to change the trajectory by a larger deflection angle than smaller planets. This can be exploited by planning a flyby with a higher energy change index (f) and ultimately a higher change in energy.

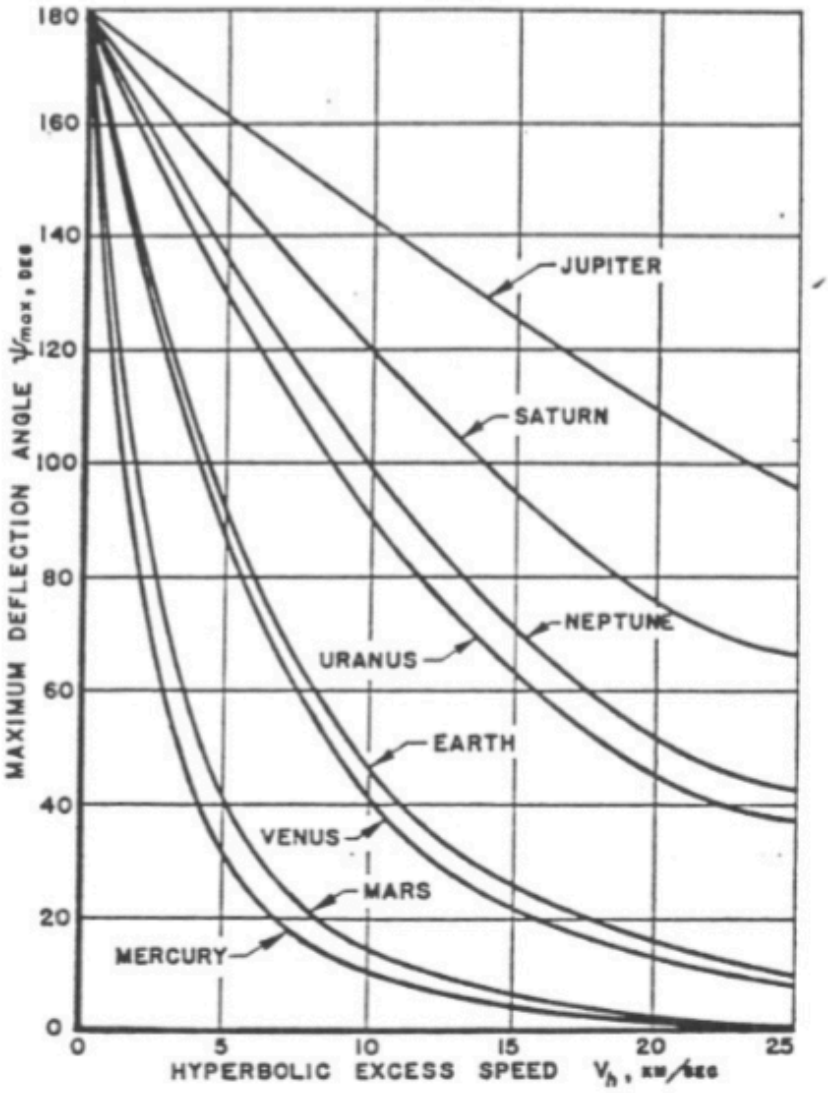

Figure 3. Maximum deflection angle vs. hyperbolic excess speed of spacecraft [3]

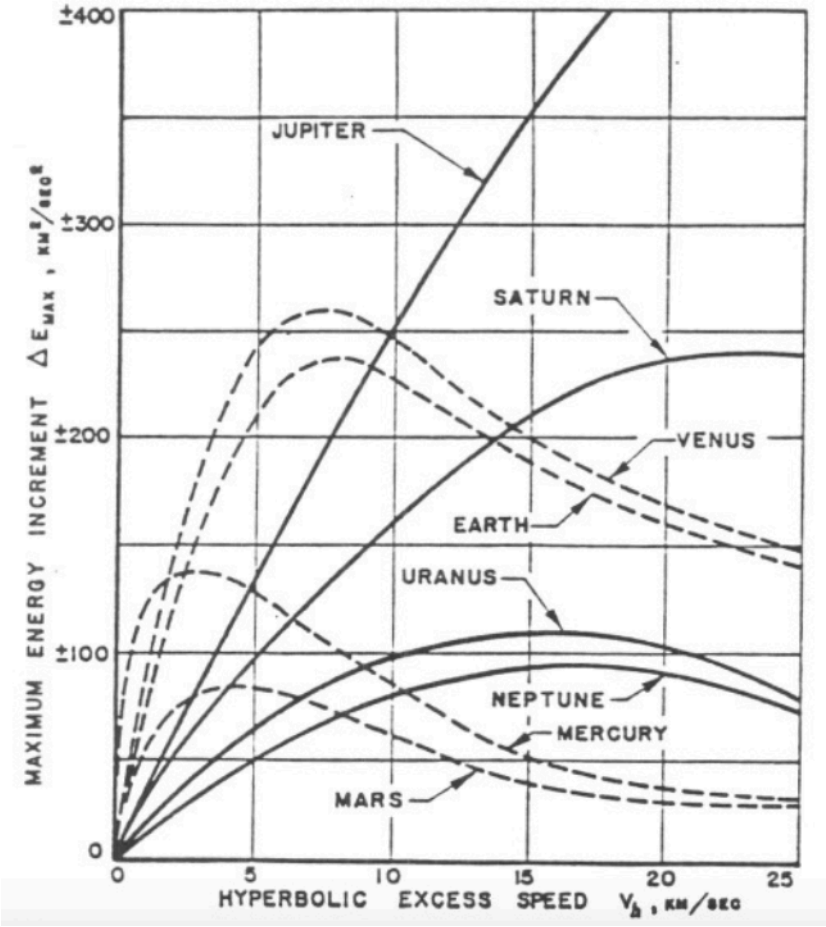

Figure 4. Maximum energy increment vs. hyperbolic excess speed of spacecraft [3]

Utilizing Jupiter Gravity Assist to Reach Trans-Neptunian Objects

A series of five papers and a poster has recently been published which survey mission opportunities to trans-Neptunian objects (TNO). [7] [8] [9] [10] [11] [12] Because of their great distance from the Sun, trans-Neptunian objects are believed to obtain characteristics that may offer clues to the formation and early beginnings of the solar system. Therefore, these objects would be worthwhile candidates for exploration missions. [7]

In the first paper, a trajectory analysis was performed. Initially, the process consisted of researching prior missions including: Voyager 1 and 2, Pioneer 9 and 10, Galileo, Cassini and New Horizons. Multi-planet flybys were considered, similar to the trajectories used by Voyager and Cassini. Single planet flybys of Jupiter and Saturn were also considered. [7]

Trajectory analysis for a mission to TNO Quaoar was performed first. Using a multi-planet flyby trajectory, the best result was a Venus-Venus-Jupiter Gravity Assist (VVJGA). This resulted in a total delta-V of 9.04 km/s and a time of flight (TOF) of 19.5 years (departing in February of 2025). These results compared poorly with the achievements of New Horizons – a total delta-V requirement of 8.92 km/s and 9.49 years TOF. Therefore, single planet flyby trajectories were studied next. Utilizing Saturn for a gravity assist resulted in a delta-V requirement of greater than 9.5 km/s and a TOF of 13.5 years for departure dates ranging from 2015 to 2040. However, Jupiter flybys produced significantly better results. For example one trajectory considered, resulted in a delta-V requirement of 7.15 km/s and a TOF of 13.57 years (launch date: November 22, 2027). The data shows that a Jovian gravity assist architecture was not only optimal for New Horizons mission but also very likely the optimal architecture for any mission to a TNO. [7] This conclusion is part of the basis for the subject and scope of this thesis.

The second paper examined orbital capture of a space vehicle upon arrival at several TNOs: Huya, Ixion, Orcus, Rhadamanthus, Salacia, Sedna, and Varuna. The primary focus was on high-thrust trajectory missions. Orbital capture results in a higher potential for scientific return than a flyby of a TNO. All trajectories considered utilized a gravity assist flyby at Jupiter. A driving factor for launch dates was based upon the orbital period of Jupiter. Launch opportunities occurred about every twelve years when Jupiter properly aligns with the selected TNO. For orbital capture to be feasible, earth departure characteristic energy (C_3) was restricted to 120 km^2/s^2. This allows for a larger payload mass and also a lower arrival V_∞ which is necessary for orbital capture. In this paper, the minimum allowable Jupiter periapse radius was set to 1.1 Jovian radii. High-thrust trajectories were examined using the Mission Analysis Environment (MAnE). [13] Figure 5 shows how time of flight influences C_3, v_∞ at arrival at the TNO and Jupiter periapsis radius. The longer time of flight means that less delta-V is required from the Jupiter flyby, allowing for a more distant flyby and ultimately less radiation exposure. [9]

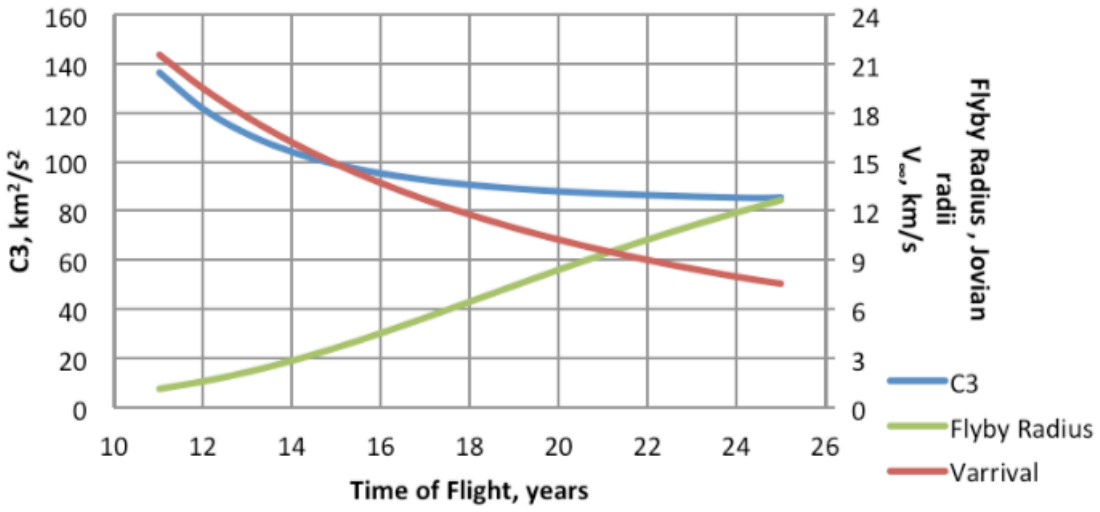

Figure 5. Jupiter Flyby Radius and Arrival V∞ vs. Time of Flight for a launch to Salacia on 26 February, 2043 [9]

The third paper examined mission opportunities to TNOs with a focus on low-thrust trajectories as well as the radiation analysis during Jupiter flybys of high-thrust trajectories. Flight paths were evaluated using MAnE and Heliocentric Interplanetary Low-Thrust Optimization Program (HILTOP). [14] Radiation environment analysis was performed on missions to Sedna, Quaoar and Makemake using the same steps, which will be later outlined in this thesis. The resulting dose depth curves are found in Figure 6. The details of the mission trajectories analyzed are listed in Table 1. [10]

The fourth paper extends the previous work with a more detailed analysis of the Jovian radiation environment during a gravity assist flyby. Dose-depth curves were calculated for both high and low-thrust missions to TNO Huya, as well as the Voyager 1 and 2 missions. Results are shown in Figure 7. [11]

Figure 8 shows a comparison of silicon radiation doses behind 5 mm of aluminum shielding as a function of transit time to TNO targets Quaoar, Huya and Haumea. While no significant advantage is seen for a high or low-thrust mission, it is apparent that radiation is more severe for faster transit times. Faster transit times require the spacecraft to fly closer to Jupiter, thereby exposing the vehicle to greater amounts of radiation. A detailed look at Jupiter flyby radius vs transit times can be seen in Figures 9 and 10 for TNO targets Huya and Quaoar, respectively. [11]

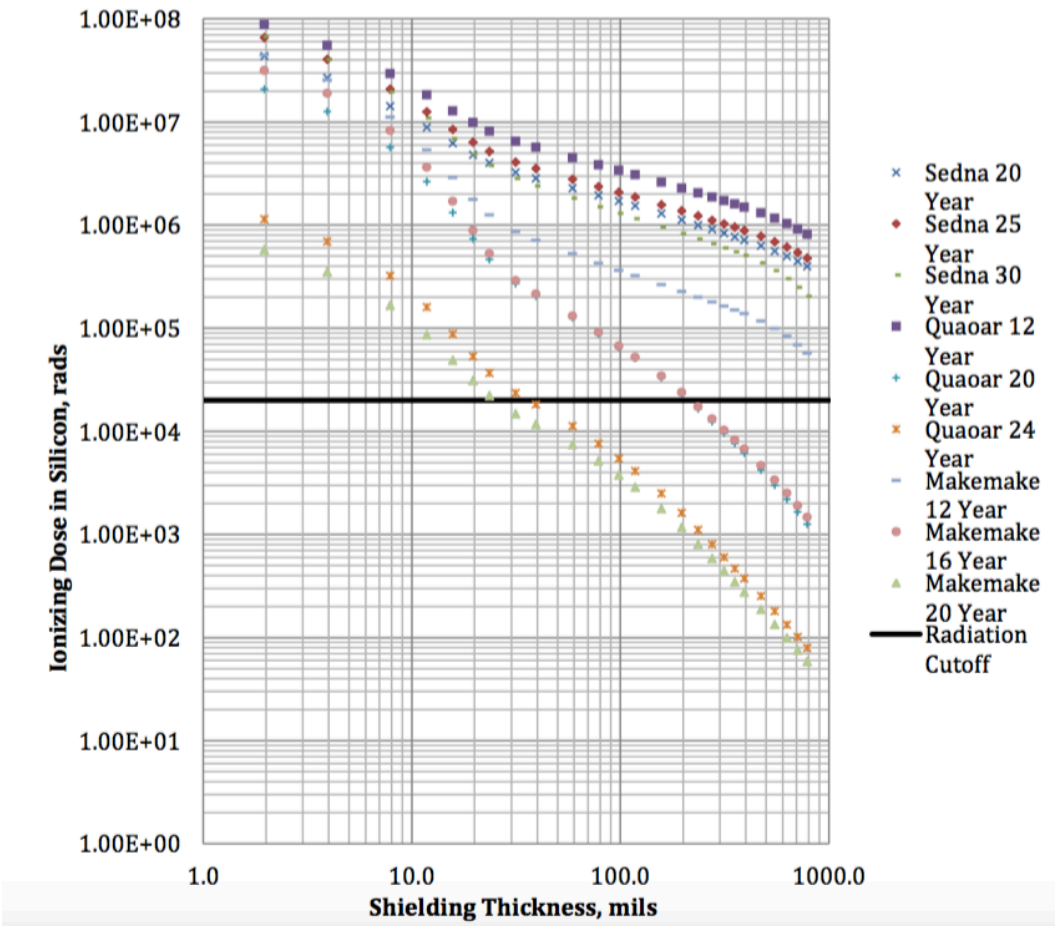

Figure 6. Radiation Dose-Depth curves for several potential missions. The "radiation cutoff" is at a level commonly used as an allowable upper limit. [10]

Table 1. Mission Details for Jovian Flyby Radiation Analysis Cases [10]

Sedna	Earth Dep. Date	Transit to Jupiter (days)	Pass Dist., (Jovian radii)	V_∞ (km/s)
20 Year	2/4/2044	482.8	1.42	13.09
25 Year	2/4/2044	569.3	3.30	10.14
30 Year	2/4/2044	621.0	5.60	8.85
Quaoar				
12 Year	24/11/2027	539.0	3.29	12.33
20 Year	1/8/2029	679.6	13.29	8.60
24 Year	22/11/2027	698.7	17.01	8.24
Makemake				
12 Year	29/9/2025	397.4	4.67	17.87
16 Year	25/9/2025	461.0	9.37	14.53
20 Year	23/9/2025	495.8	14.37	13.07

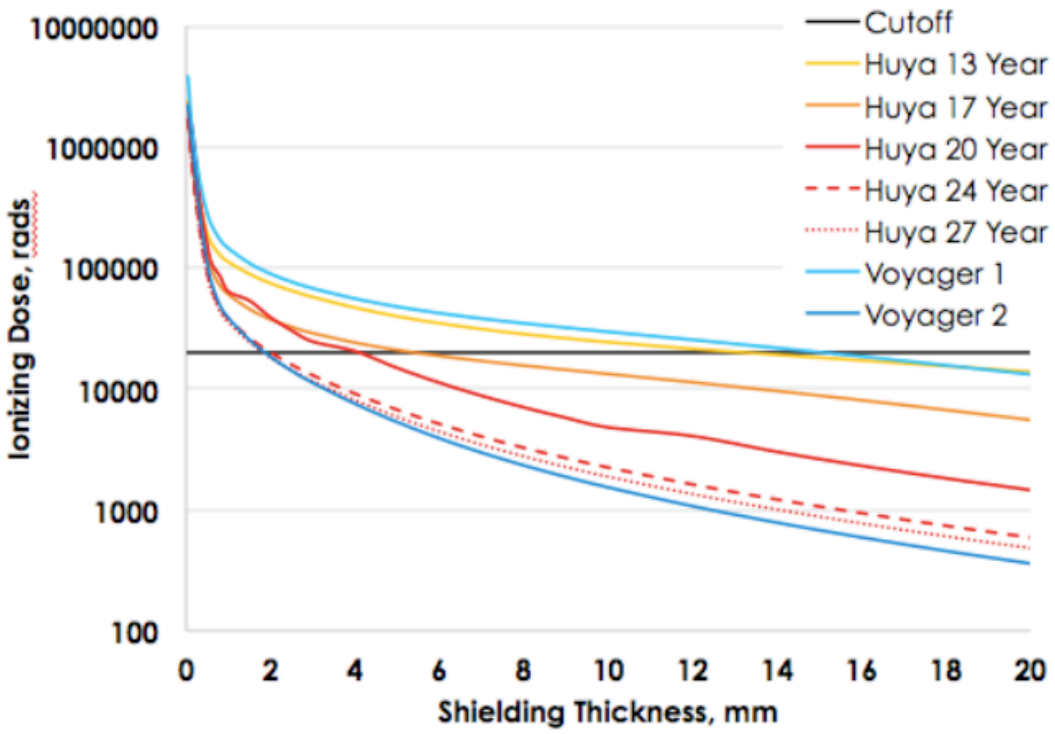

Figure 7. Jovian flyby radiation environment for a 2026 departure to Huya with Voyager flyby radiation for comparison. The "radiation cutoff" is at a level commonly used as an allowable upper limit. [11]

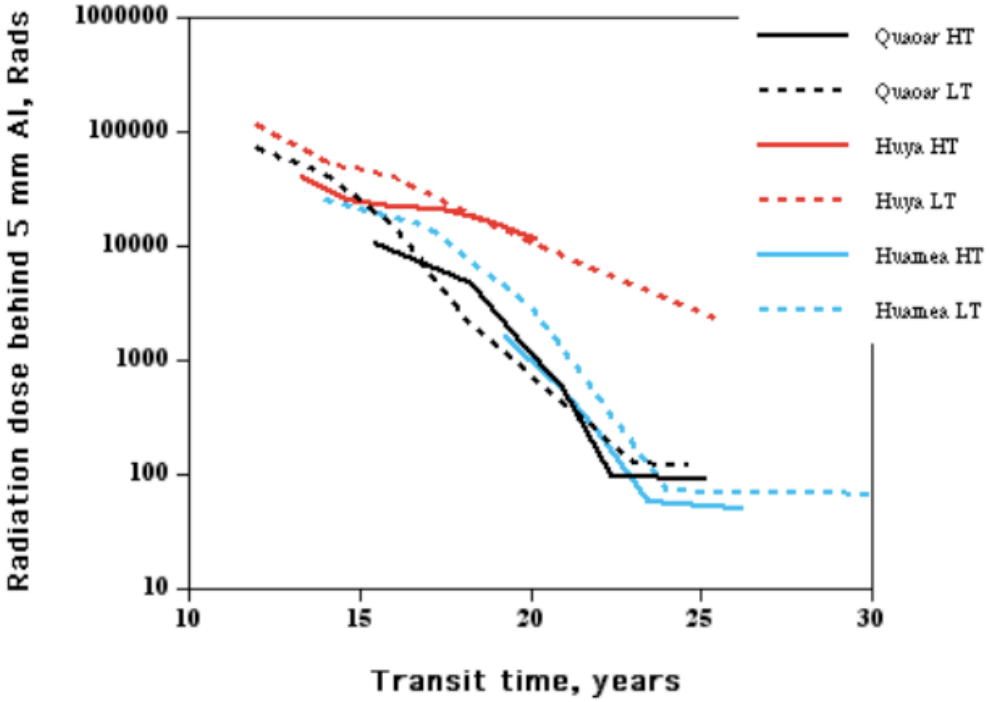

Figure 8. Radiation dose behind 5 mm of aluminum shielding for low and high thrust missions to Huya, Quaoar and Haumea [11]

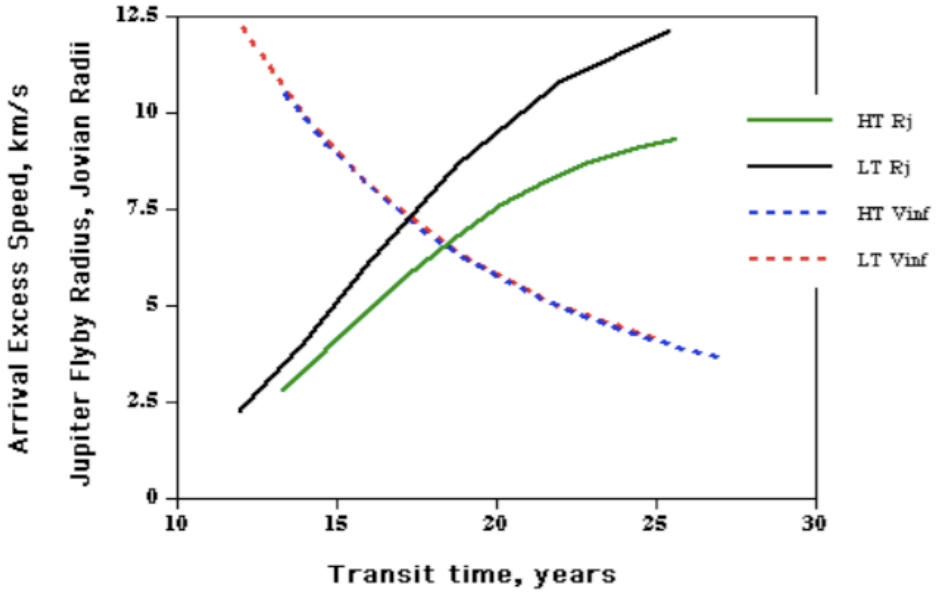

Figure 9. Arrival hyperbolic excess speed at the target and Jupiter flyby radius as a function of transit time for high and low-thrust missions to Huya [11]

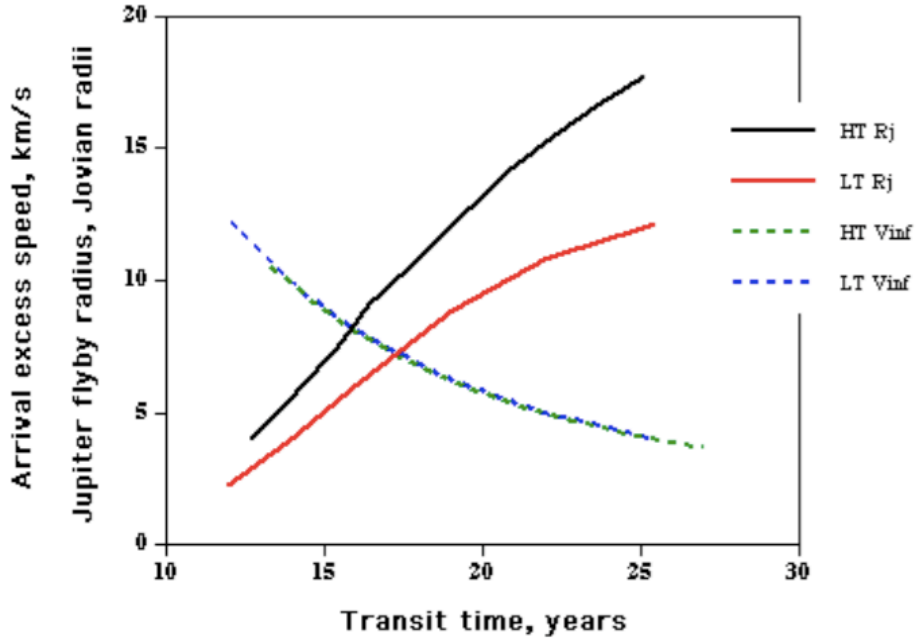

Figure 10. Arrival hyperbolic excess speed at the target and Jupiter flyby radius as a function of transit time for high and low-thrust missions to Quaoar [11]

CHAPTER III
HISTORICAL JUPITER FLYBYS

To date, there have been seven different spacecraft that have flown by Jupiter. Each of these missions faced challenges due to the planet's harsh radiation environment. Below is a summary of each spacecraft's journey to deep space.

Pioneer

The Pioneer program began in 1957 when the government authorized the launching of small unmanned spacecraft towards the moon. Several Pioneer spacecraft were launched for exploration purposes. In 1968, the Space Science Board of the National Academy of Sciences stated that Jupiter would be the most interesting planet to study and that it was now technically feasible to send a spacecraft to study it. The Board recommended that two exploratory probes in the Pioneer class be launched towards Jupiter. Several scientific papers were presented about exploration to the outer planets, including information regarding utilizing gravity assists. NASA completed studies that showed that the gravitational field of Jupiter could accelerate spacecraft to speeds that would enable them to travel to the outer planets. This study recommended that two spacecraft be launched towards Jupiter in 1972 and 1973: Pioneer 10 and 11. The idea was that when each spacecraft flew by Jupiter it would obtain enough additional energy to carry it outside the solar system. Additionally, the probes would be equipped to collect data on the Jovian radiation environment. Figure 11 shows the trajectory of both missions; each tick mark represents one Earth year. [15]

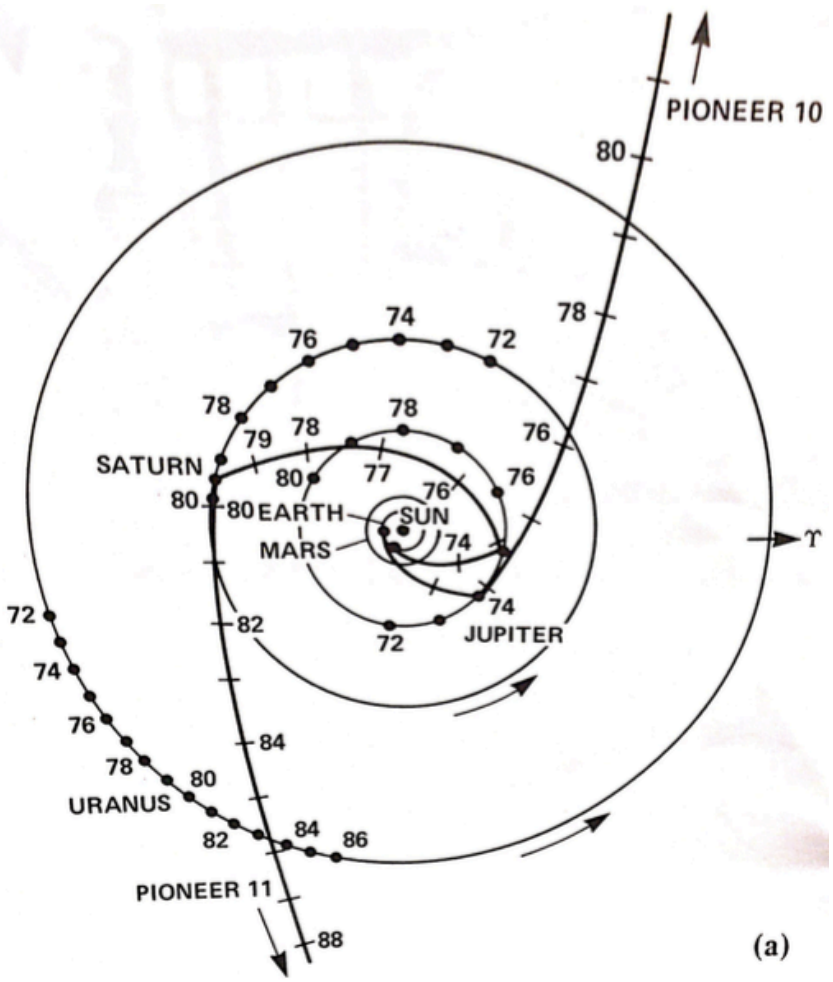

Figure 11. Sun-centered trajectories of Pioneer 10 and 11. [15]

Pioneer 10

Pioneer 10 was launched on 2 March 1972 with a primary mission to study Jupiter's atmosphere, magnetosphere and satellites. The spacecraft flew by Jupiter with a periapsis altitude of 1.86 Jovian radii (R_J) or 132,804 km (1 R_J = 71,400 km) in December 1973. The encounter trajectory was chosen to provide the maximum information about the radiation environment of Jupiter to smallest feasible radial distance. This decision was made knowing that the risk of radiation damage could end the mission at Jupiter. Scientists wanted to know how closely a spacecraft could safely approach Jupiter in order to take advantage

of the gravity slingshot effect without damaging the spacecraft's electrical and optical equipment. Answering this question was one of the primary objectives of the mission.[15] The spacecraft received a huge gravitational assist from the flyby, with a total velocity gain of 12.6 km/s. Upon arrival at Jupiter, the heliocentric velocity of Pioneer 10 was 9.8 km/sec. After the flyby, the spacecraft's heliocentric velocity had jumped to 22.4 km/s. [16]

Pioneer 10 was the first spacecraft to travel through the Asteroid Belt and also the first to observe an outer plant. During the Jupiter flyby, Pioneer 10 obtained the first-ever close-up image and discovered that Jupiter is a liquid planet. The radiation effects of Jupiter caused some bit flips on the system, resulting in some data and images being lost. After the flyby, the spacecraft went on to explore the outer regions of the solar system. [15]

Pioneer 11

Pioneer 11 was launched on 5 April 1973 with a mission to study the interiors, atmospheres, moons and rings of both Jupiter and Saturn. The spacecraft flew by Jupiter at a periapsis altitude of 42,840 km (0.6 R_J) on 2 December 1974. The trajectory was highly inclined (51.8 degrees) to the Jovian equator. The spacecraft returned approximately 460 images of Jupiter and its Galilean satellites from 18 November through 9 December 1974. A day before periapsis, a malfunction caused by radiation affected the telescope on board. Some images were lost before a workaround could be put in place. For planetary astronomers, the image of the Great Red Spot of Jupiter was one of Pioneer 11's most exciting results. Previously, the highest resolution image of the Great Red Spot taken by Pioneer 10 was degraded due to radiation problems. [15]

Voyager

In 1964, Dr. Gary Flandro discovered a rare geometric alignment of the outer planets that occurs every 175 years. He conceived the Grand Tour multi-planet mission utilizing a gravity assist technique that would reduce flight durations

from 40 years down to less than 10 years. His work led to the success of the Voyager missions. Later, in 1965, Dr. Flandro studied gravity assist trajectories to Pluto, these trajectories were the basis for the New Horizons mission, which flew by Pluto in July 2015. [5]

Together, Voyager 1 and 2 took more than 33,000 pictures of Jupiter and its five major satellites. Discovery of active volcanism on the satellite Io was the greatest unexpected finding. It was the first time active volcanoes had been seen on another body in our solar system. [17] Figure 12 shows a heliocentric view of both Voyager trajectories. [18]

Voyager 1

Voyager 1 launched on 5 September 1977 with a mission to study Jupiter and Saturn. Voyager 1 reached its closest approach to Jupiter on 5 March 1979 at an altitude of 276,807 km. [17] Figure 13 shows the heliocentric speed of Voyager 1 during the Jupiter flyby, with the max speed obviously occurring at periapsis. As one can see in the chart, there was a heliocentric velocity gain of 10.8 km/s. [19] Voyager 1 is currently in "interstellar space."

Voyager 2

Voyager 2 launched on 20 August 1977, also with a mission also to study Jupiter and Saturn. Voyager 2 reached its closest approach to Jupiter on 9 July 1979 at an altitude of 650,270 km. Figure 14 shows the heliocentric velocity of Voyager 2 as it traveled through the solar system. One can see the increase in velocity caused by each planetary flyby. The flyby at Jupiter resulted in a 12 km/s velocity gain. [19] Voyager 2 went on to explore Uranus and Neptune and is still the only spacecraft to have visited these outer planets. Voyager 2 is currently in the "Heliosheath" – the outer layer of the heliosphere where the solar wind is slowed down by interstellar gas. [17]

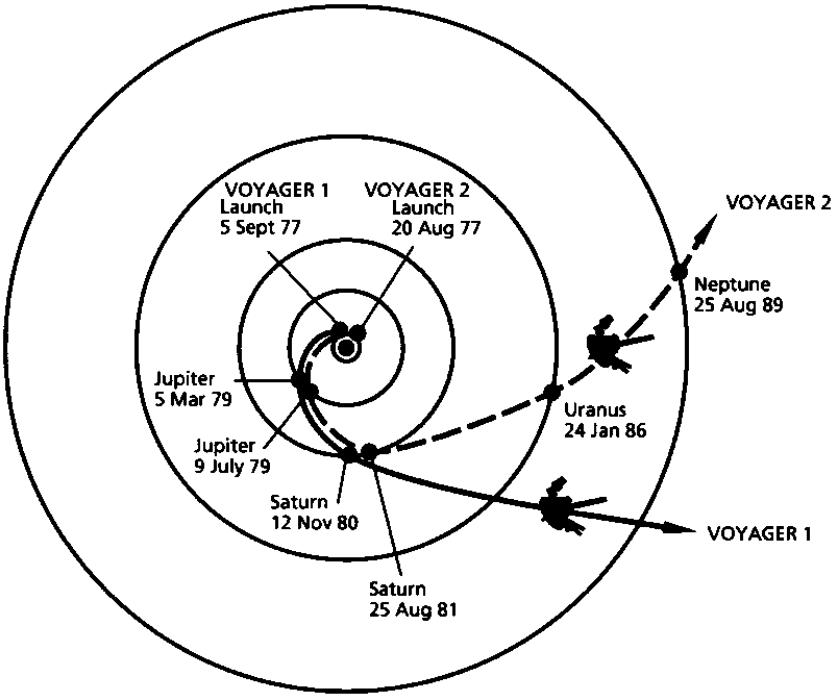

Figure 12. Heliocentric view of Voyager trajectories [18]

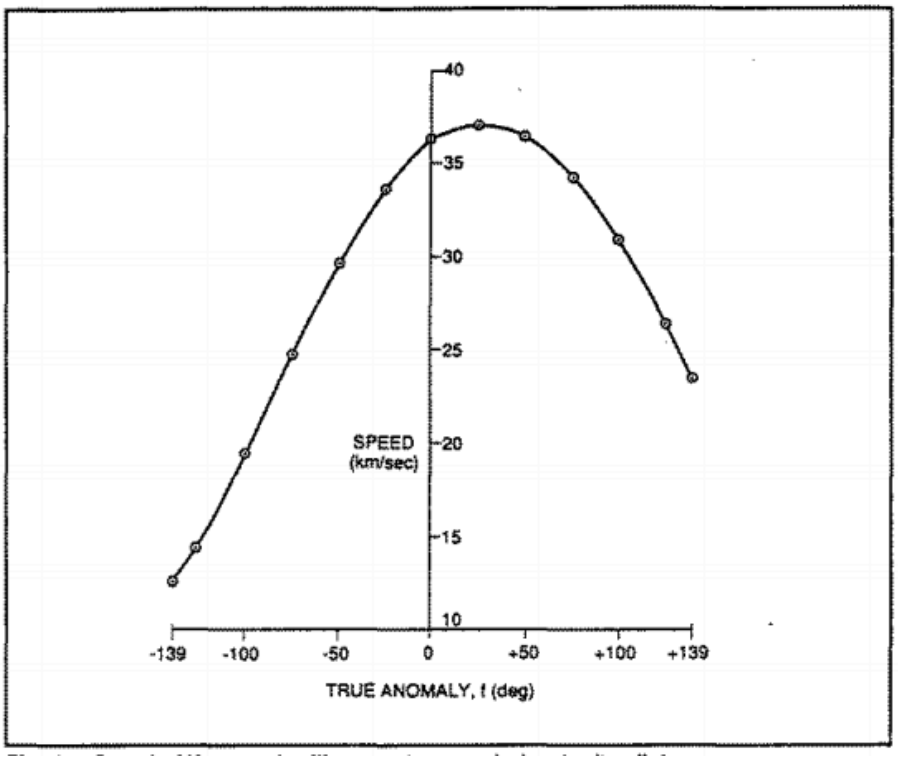

Figure 13. Heliocentric speed of Voyager 1 during Jupiter Flyby [19]

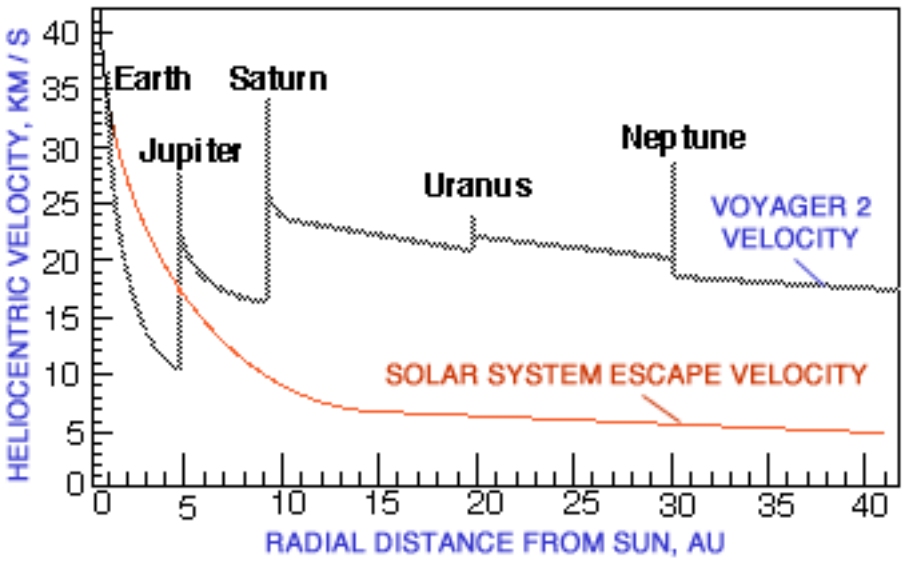

Figure 14. Heliocentric velocity of Voyager 2 versus distance from the Sun. [20]

Ulysses

Ulysses launched on 6 October 1990 as a joint mission between ESA and NASA. The primary objective was to study the inner heliopshere in three dimensions. The primary purpose of its Jupiter flyby was not to achieve an increase in velocity (like Voyager) but rather to achieve a significant change in heliocentric inclination. The goal of the gravity assist was to place Ulysses in its final heliocentric out-of-ecliptic orbit in order to pass over the poles of the Sun. [21] Post JGA, the flight path of Ulysses was bent 80 degrees southward from the heliocentric ecliptic plane. [22] The mission profile of Ulysses is displayed in Figure 15. The spacecraft reached its closest approach with Jupiter on 8 February 1992 at a periapsis altitude of 6.3 Rj (379,134 km). The inbound trajectory was similar to the missions before it, however Ulysses reached high latitudes of ~40 degrees north of the Jovian equator during periapsis. This is displayed in Figure 16. Another unique aspect of the trajectory was the journey through the Io Plasma Torus (IPT). The opportunity to study Jupiter's magnetosphere was utilized and observations confirmed and complemented the findings of the previous four missions. [21]

Cassini

Cassini launched on 15 October 1997 with a primary mission to explore the Saturn System. Cassini's flyby of Jupiter occurred on 30 December 2000 at an altitude of 136 R_j (9,721,846 km) and provided the final push to get the spacecraft to Saturn. The Galileo orbital mission was ongoing during the flyby and presented a unique opportunity – to study Jupiter simultaneously with two different spacecraft. [24] Figure 17 outlines the mission trajectory; the primary purpose of the Jupiter flyby was to provide Cassini with a final boost to Saturn. [25] Cassini's heliocentric velocity before the Jupiter gravity assist was 11.6 km/s and afterward increased to a velocity of 13.7 km/s for a total gain of 2.1 km/s. [26]

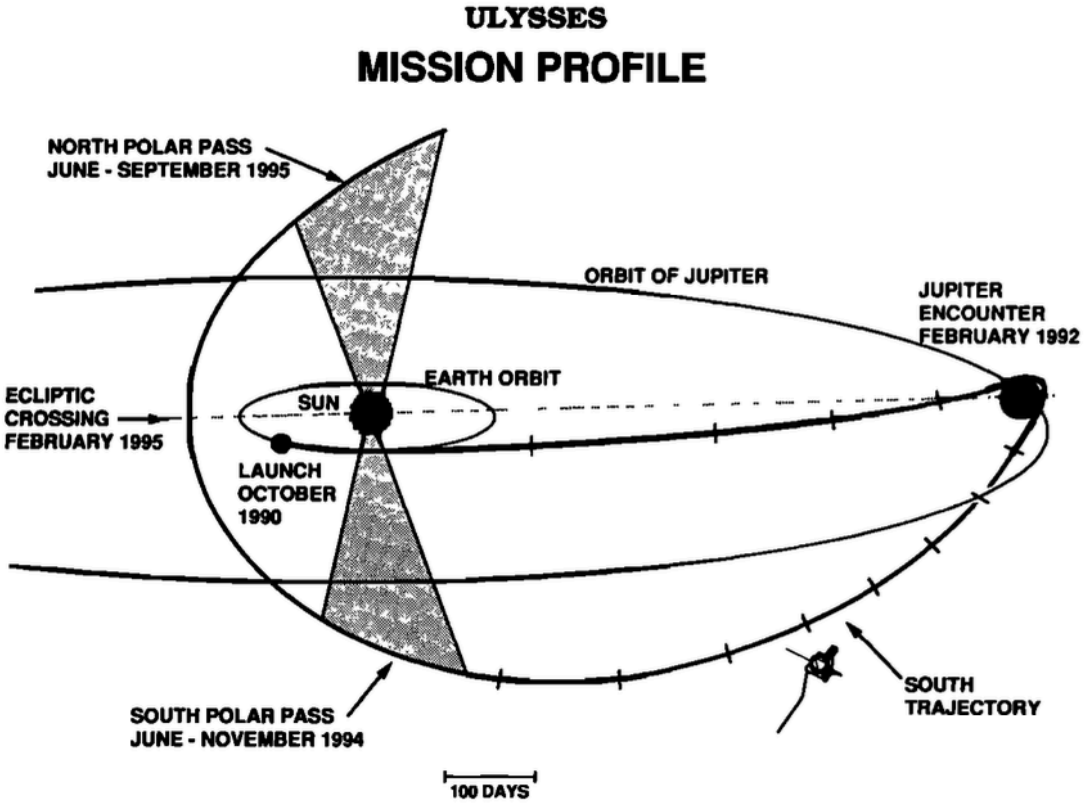

Figure 15. Profile of the Ulysses mission as represented by the trajectory. The trajectory consists of two ellipses, one that carried the spacecraft from the Earth to Jupiter and the other highly inclined to the ecliptic plane and passing over the sun's polar regions. [23]

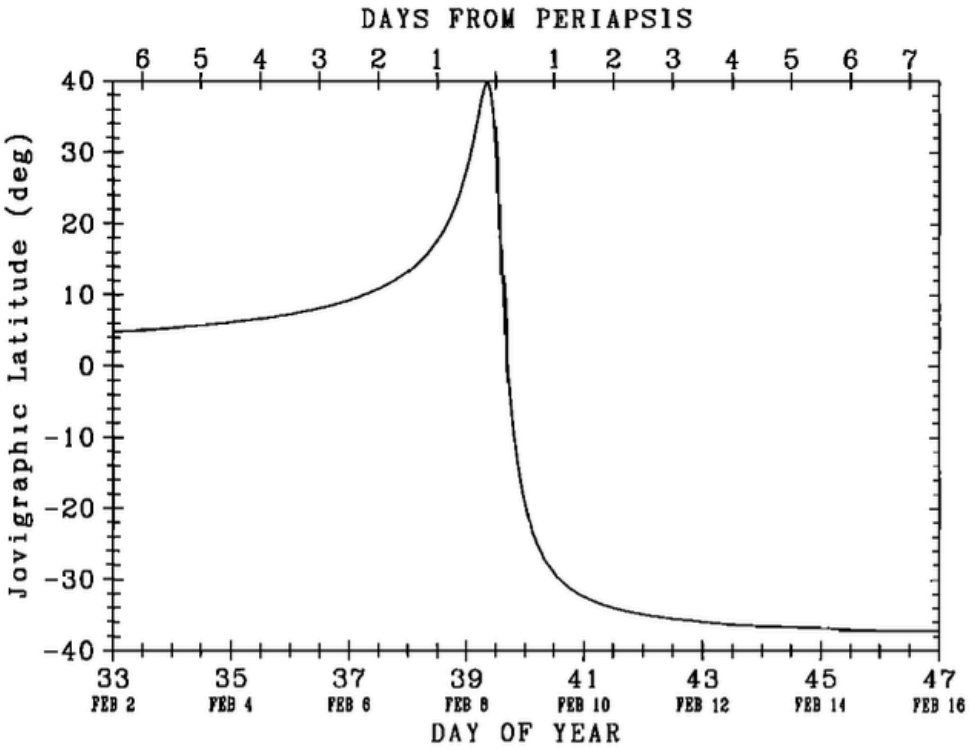

Figure 16. Jovigraphic latitude of Ulysses during encounter [23]

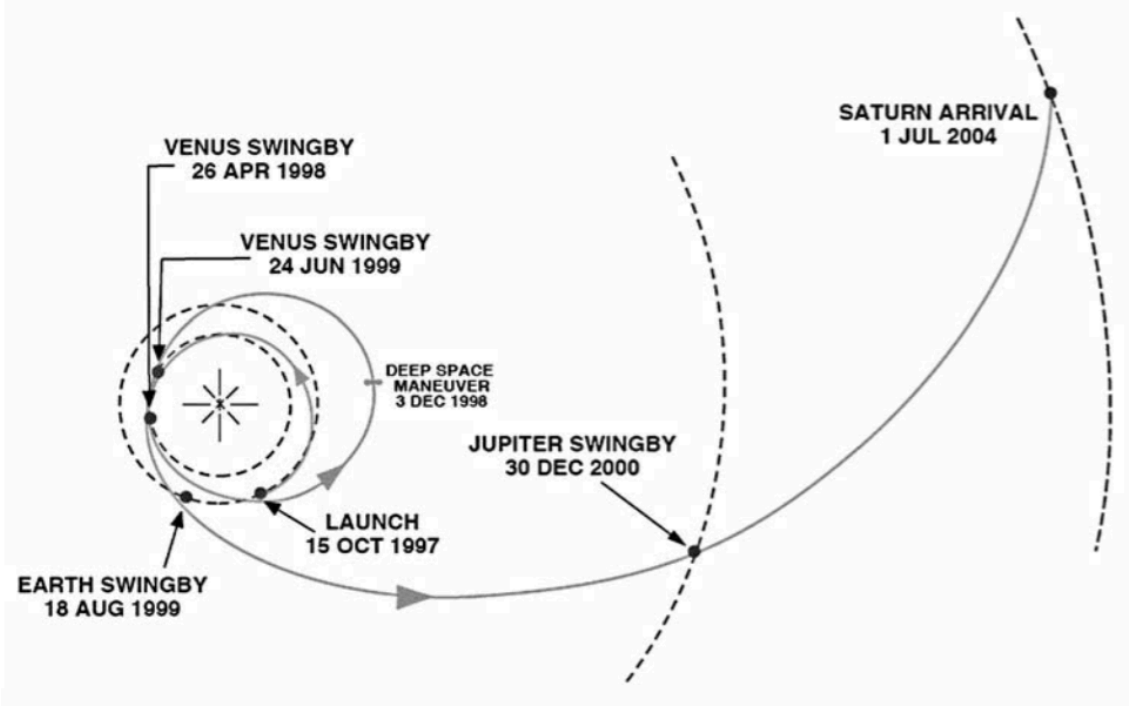

Figure 17. Cassini Mission Cruise Trajectory [25]

New Horizons

New Horizons is a NASA mission that provided the first-ever reconnaissance of Pluto and its moons. The spacecraft launched on 19 January 2006 and reached Pluto on 14 July 2015. New Horizons received a gravity assist during a flyby of Jupiter on 28 Feb 2007 with a periapsis radius of 32 R_J (2,237,152 km). During its flyby of Jupiter, New Horizons became the first spacecraft to cross the Jovian magnetotail. [1] More information about New Horizon's trip down the magnetotail will be discussed in Chapter IV. New Horizons is currently exploring the Kuiper belt.

Figure 18 shows the interplanetary trajectory of New Horizons. The purpose of the flyby at Jupiter was to inject a speed boost necessary for the spacecraft to reach Pluto. Figure 19 shows the heliocentric speed of the spacecraft versus its distance from the Sun. One can see that the highest heliocentric speed is at the beginning when the spacecraft is launched into its trajectory. The speed decreases until it reaches Jupiter, where a velocity gain of 3.83 km/s occurs. After the JGA, the spacecraft speed steadily decreases. During the Pluto flyby, there is a small gravity assist but the magnitude is minimal and is not visible in Figure 18. [27]

Summary of Missions

Table 2 summarizes all Jupiter flybys to date. Some data is missing because it is not available.

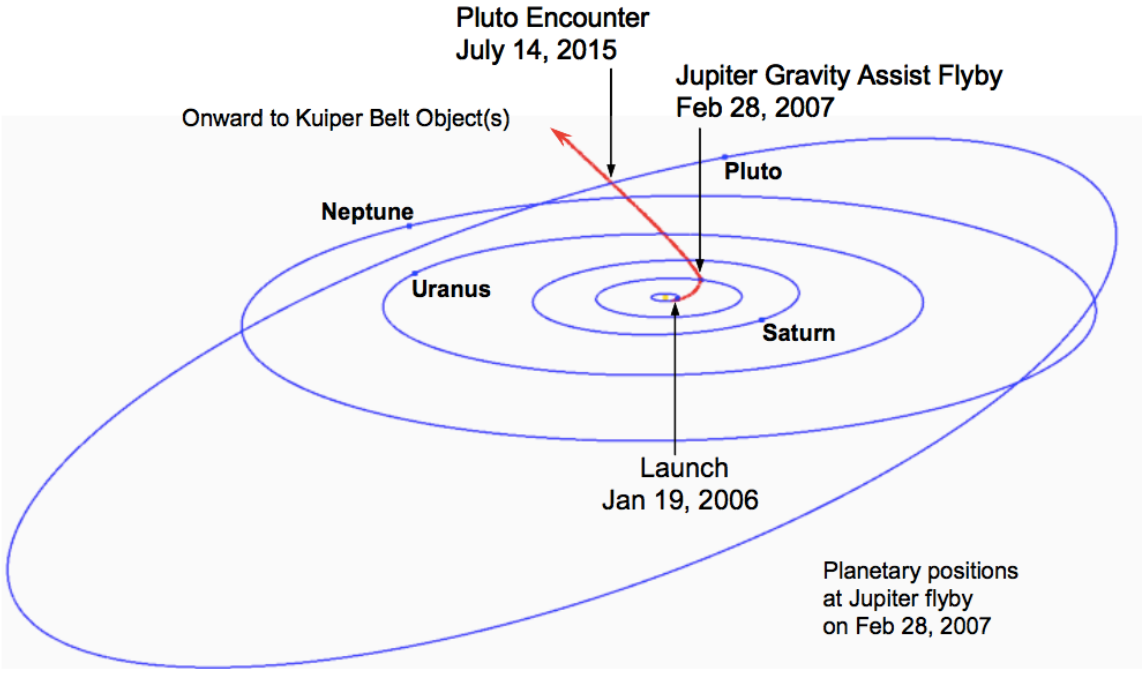

Figure 18. New Horizons Mission Trajectory [27]

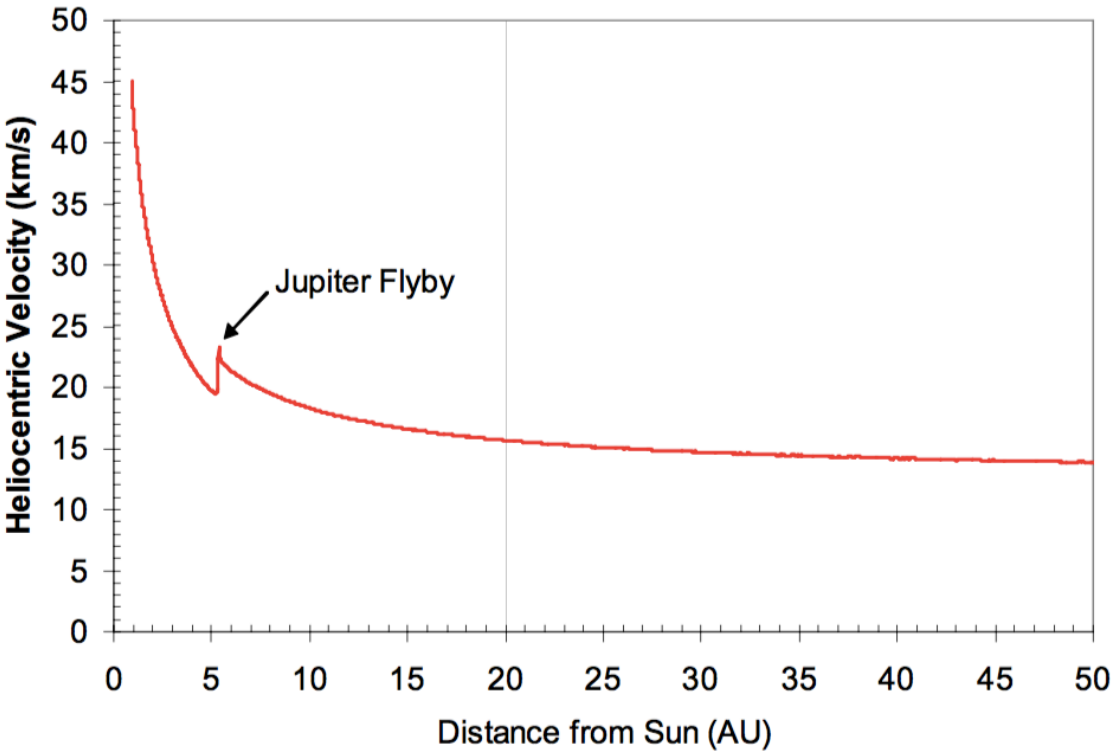

Figure 19. Heliocentric velocity of the New Horizons Spacecraft vs. distance from the Sun [27]

Table 2. Summary of all Jupiter Flybys to Date.

Mission	Flyby Date	Periapsis Altitude	Heliocentric Velocity Gain From Flyby	Destination
Pioneer 10	Dec 1973	132,804 km	12.7 km/s	Jupiter
Pioneer 11	Dec 1974	42,840 km	----	Asteroid belt/Jupiter, Saturn, Solar winds, cosmic rays
Voyager 1	Mar 1979	276,807 km	10.8 km/s	Jupiter, Saturn, Outer solar system/interstellar space
Voyager 2	Jul 1979	650,270 km	12 km/s	Jupiter, Saturn, Uranus, Neptune
Ulysses	Feb 1992	379,134 km	----	Sun (high inclination)
Cassini	Dec 2000	9,507,896 km	2.1 km/s	Saturn
New Horizons	Feb 2007	2,237,152 km	3.83 km/s	Pluto

CHAPTER IV
JOVIAN RADIATION ENVIRONMENT

In order for a radiation belt to form around a planet, it must have a magnetic field. The magnetic field deflects charged particles that are traveling to the planet via solar winds (a stream of ionized particles constantly departing the sun). This creates a cavity that protects the planet against the harsh environment of particle radiation. Mercury, Earth and each of the four gas planets (Jupiter, Saturn, Uranus and Neptune) all have magnetospheres. [28] Venus and Mars are the only planets with almost a nonexistent magnetic field and therefore, no radiation belt. [28]

Jupiter is roughly 10 times larger than Earth in radius, but it's magnetic moment is 10^5 times larger. Since, at the equator, the magnetic field is approximately proportional to the magnetic moment divided by the cube of the planet's radius, the Jovian magnetic field is approximately 20 times stronger than Earth's. [29]

Magnetosphere

A magnetosphere is a field of influence around a planet where the forces of the magnetic field of that planet are strong enough to divert solar wind. This creates a space of hot plasma derived from either the solar wind or the planet. To maintain a magnetosphere, three components are required: a magnetic field that can divert solar wind, a source of plasma and a source of energy. There are two types of magnetospheres: solar-wind driven and rotationally driven. The Earth is an example of a solar-wind driven magnetosphere; plasma and energy are derived mainly from the solar wind. Jupiter's magnetosphere is a rotationally driven magnetosphere; the bulk of the energy is derived from the planet's rotation and the plasma is derived from the planet and surrounding satellites. [30]

Jupiter's intense magnetic field and fast rotational period (approximately 9 hours and 55 minutes) create an enormous magnetosphere. Jupiter's magnetosphere differs from most other magnetospheres since it derives most of its plasma from Jupiter's moon Io. It is estimated the plasma torus created by Io is located between the radial distances of 5.2 to 10 Rj and contains several million tons of plasma. [30] Figure 20 depicts the magnetosphere of Jupiter.

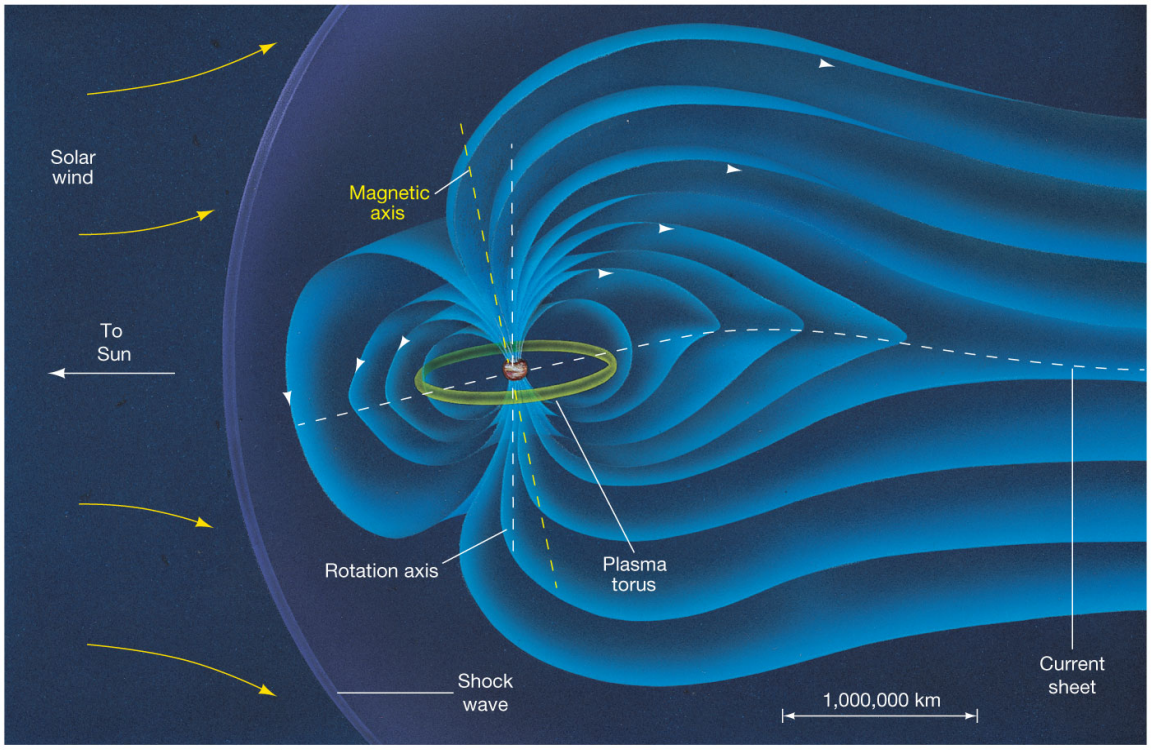

Figure 20. Jupiter's Magnetosphere [31]

Magnetotail

The magnetosphere of a planet is compacted on the side nearest the sun, and it is immensely stretched on the farthest side, forming a region known as a magnetotail. Since Jupiter's magnetic field is the largest in our solar system, so is its magnetotail. The tail extends away from the sun and reaches farther than

Saturn's orbit, as seen in Figure 21. It was measured to be at least 500 million km anti-sunward from Jupiter during Voyager 2's trip to Saturn. [32]

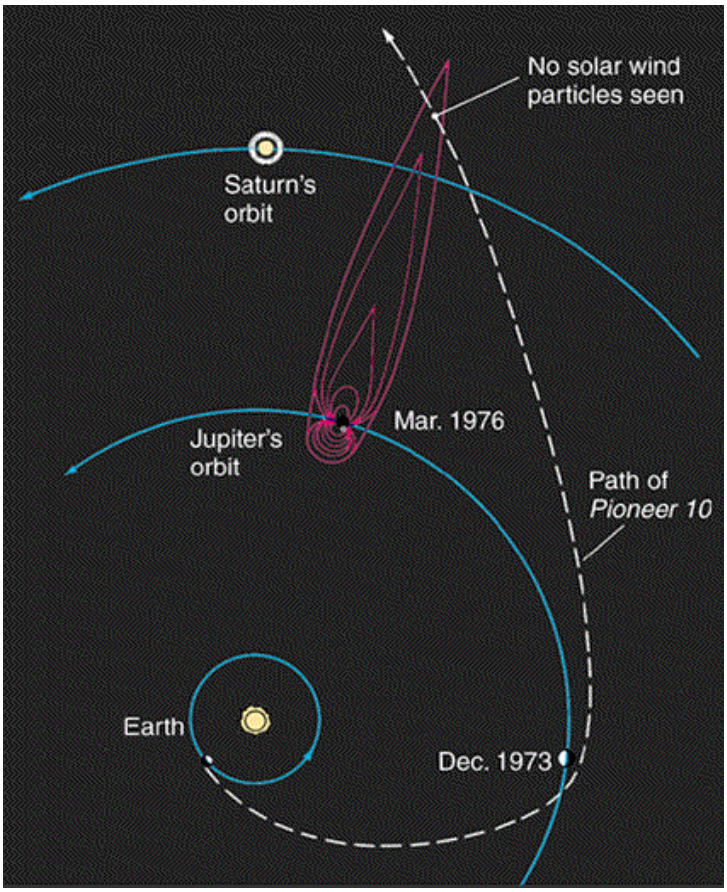

Figure 21. Heliocentric view of Jupiter's magnetosphere and the flight path of Pioneer 10 [31]

In 2007, the New Horizons spacecraft crossed the magnetotail of Jupiter while on its way to Pluto. Previous missions to Jupiter have revealed that Io is the most significant factor in the development of the Jovian magnetosphere. Io produces about 1 metric ton of sulfur dioxide (SO2) per second. The sulfur dioxide material is partially ionized and partially transported into the magnetosphere of Jupiter. Magnetic field lines are therefore loaded with S and O ions that form a plasma disk around Jupiter. The disk wobbles with every rotation of Jupiter and stretches as it is loaded with more and more ions. As it is loaded, it reaches a limit. Once this limit is reached, plasma is released into the magnetotail in the

form of a magnetic bubble called a plasmoid. This is depicted in Figure 22 below. The solar wind collides with the magnetic field of Jupiter (represented by the red dot) and creates a bow shock. A magnetosheath is formed around the planet as well as an extended magnetotail. Plasma from the moon Io (orbit is displayed as blue arrows) and from other sources is ejected down the tail. The magnetic boundary between the planet's magnetic field and the solar wind is called the magnetopause._ [28]

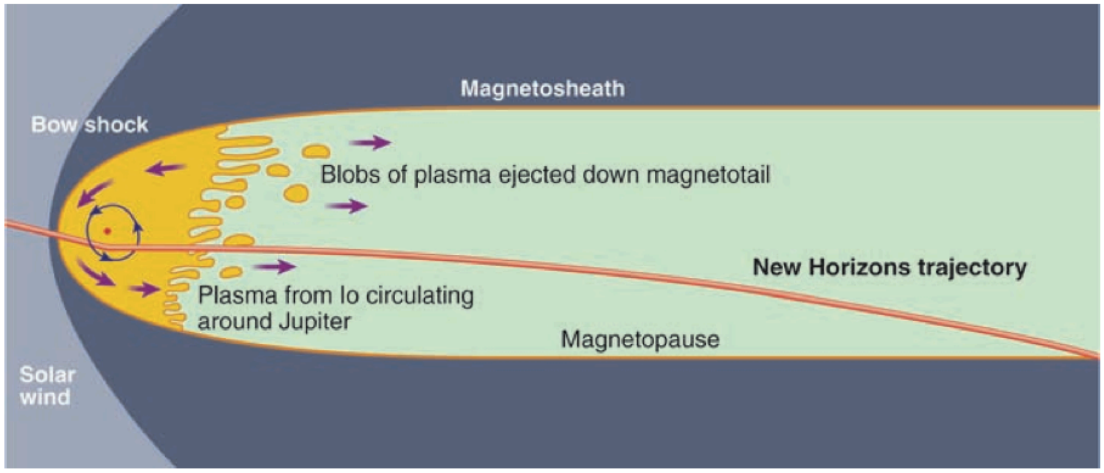

Figure 22. Jupiter's plasma environment and the trajectory of New Horizons spacecraft. [28]

New Horizons followed a nearly ideal trajectory for magnetotail observations and revealed many surprises. Figure 23 shows the plasma observations from just after New Horizon's inbound crossing of Jupiter's magnetopause on day of year (DOY) 56 through the closest approach (~32 Rj) and back down the magnetotail to DOY 170. This diagram shows the plasma disk near Jupiter and notional large plasmoids (colored) moving down the tail between 200 and 2500 R. It also was discovered that plasmoids are not only filled with S and O ions from Io but H3+ and H+ from Jupiter. [32].

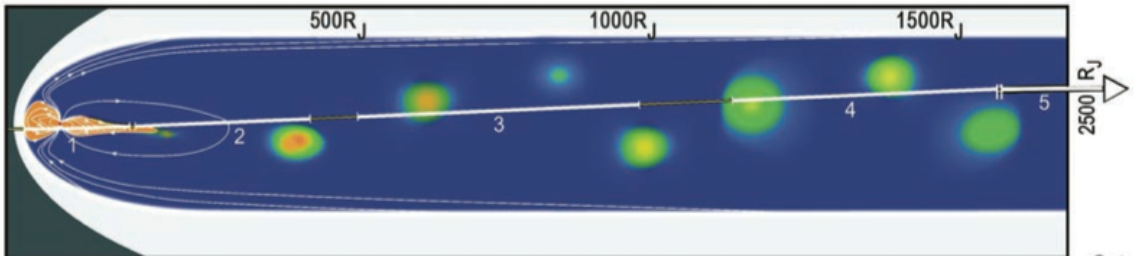

Figure 23. Jupiter plasma observations seen by New Horizons [32]

Radiation Effects on Spacecraft Electronics

Due to the harsh radiation environment of space, space vehicle electronics have a history of power resets, system failures and entering into safe mode. All spacecraft are vulnerable to the effects of radiation. There are two ways that radiation can do harm: Single Event Effects (SEE) or Total Ionizing Dose (TID). SEEs are cause by one single energetic particle while TID is a measure of how much radiation the electronic systems have received over the spacecraft's lifetime. To protect electronic systems, several safeguards may be used including shielding and redundant parts/configurations. [33]

Jovian Trapped Particle Environment

The Jovian trapped particle environment is much higher in energy and flux density than any other planets in our solar system. Trapped particles are about ten times more energetic than particles found in Earth's radiation belts. [34] The intensity of Jovian radiation belts is therefore also greater than other planets in our solar system. Divine and Garret used particle measurements from Pioneer 10 & 11 and Voyager 1 & 2 to develop the first Jupiter trapped radiation environment model. This model is named the Divine and Garrett Model (D&G83). [29] It will be discussed again in Chapter V, Methodology. Later, Garrett developed an updated electron model based on Galileo measurements and previous Pioneer measurements. This model is called Galileo Interim Electron Environment (GIRE) and will also be discussed in further detail in Chapter V, Methodology. [35]

The most dominant trapped particles at Jupiter are electrons with energy (E) in the $1 > E > 100$ MeV range. Electrons can contribute to spacecraft surface charging and damaging arcing. Electrons also can contribute to ionizing doses through direct energy deposition. Protons are the main contributors to ionizing

doses and are the leading cause of single-event upsets (SEU). SEUs appear as a soft error on spacecraft and non-destructive. They usually appear as bit flips or as other types of errors in the downlinked telemetry. [34] The figures below represent the Jovian equatorial and longitudinal proton and electron fields using the GIRE 2003 model.

Figure 24 shows the equatorial plane proton (left) and electron (right) flux in units of $\log_{10}(cm^{-2}s)^{-1}$. Figure 25 shows the longitudinal plane proton (left) and electron (right) flux in units of $\log_{10}(cm^{-2}s)^{-1}$. In both figures, the black dots represent the orbits of the Jovian moons Io, Europa, Ganymede, and Callisto (from smallest orbit to largest). Rj is the radius of Jupiter, which is equal to 71,400 km. [29]

From these figures, one can see that the proton field is limited to the two innermost most moons of Jupiter, Io and Europa. However the electron field extends far beyond the fourth moon, Callisto, and down the magnetotail. One can also see that both the proton and electron fields are asymmetrical in the equatorial plane (along 120 E and 210 E longitudes). [29] Additionally, both the proton and electron fields are somewhat flattened in the longitudinal plane. This is why flybys with high inclination will receive lower doses of radiation. [10]

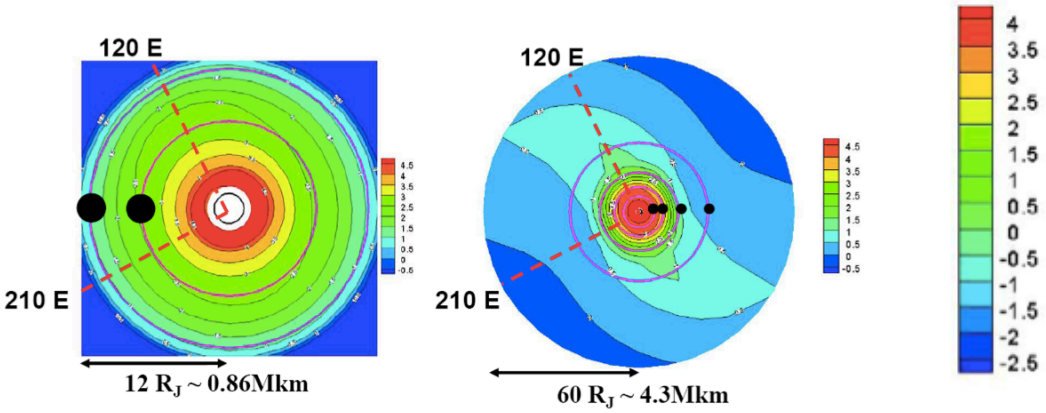

Figure 24. Jupiter trapped (GIRE 2003) equatorial plane protons (left) and electrons (right) [29]

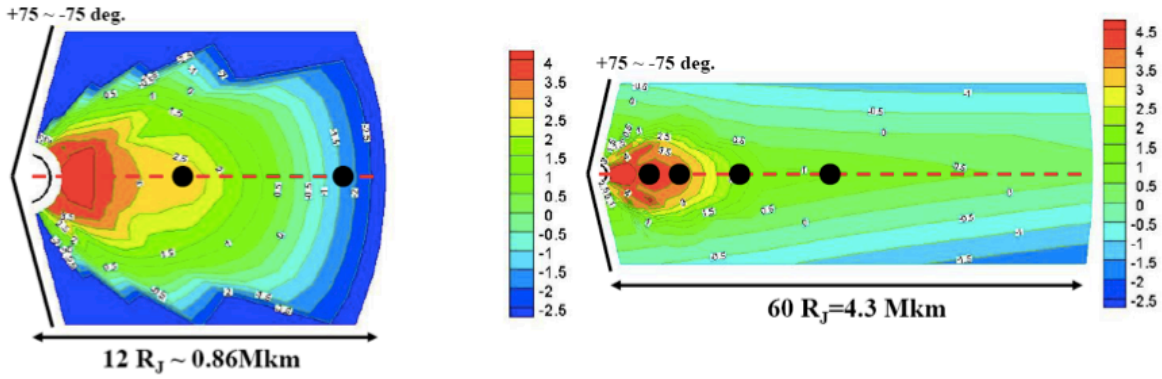

Figure 25. Jupiter trapped (GIRE 2003) longitudinal plane protons (left) and electrons (right) [29]

CHAPTER V
METHODOLOGY

The idea behind this thesis is to build a database that can be quickly used to estimate radiation dosages encountered during a Jupiter flyby. Flyby trajectories from previous missions were used as a guideline to choose bounds for building the database. Dosage as a function of four parameters was studied: inclination (inc), longitude of the ascending node (LAN), energy and altitude at periapsis (AltP). Argument of periapsis (ArgP) was briefly evaluated in one case but will require future investigation.

Software

POST

The first step in the process was to populate the desired flyby trajectories with varying parameters as listed above. To achieve this, NASA's Program to Optimize Simulated Trajectories (POST) was utilized. It provides the capability to optimize and target trajectories for space vehicles near an arbitrary planet. [36] POST is a highly validated, industry standard code for trajectory calculations. A script was written in MATLAB to automate the various parameter input values to be run. POST was used to generate a total of 16,416 flyby trajectories, showing three-dimensional position versus time (with a time step of 10 seconds). The output trajectories were saved in the format of text files for further analysis. The parameters used during the runs are listed in Table 3.

These parameters were chosen for various reasons. Initial inclination was bounded between 0° -90°. The range from 90°-180° was not considered, since one can assume it would be a mirror image. Initial LAN was not bounded; values between 0° to 360° were represented. Energy was chosen based on a range of realistic V_∞ values: 5.66 km/s to 16.5 km/s. Altitude at Periapsis was selected based on values from previous missions ranging from 1.43 R_j to 25.75 R_j.

Table 3. Trajectory Parameters

Inclination (degrees)	Longitude of Ascending Node (degrees)	Energy (km^2/s^2)	Altitude at Periapsis (km)
5	10	16.0178	100000
10	30	21.125	200000
20	50	28.125	300000
30	70	36.125	400000
45	90	45.125	600000
60	110	55.125	800000
75	130	66.125	1000000
85	150	78.125	1400000
	170	91.125	1800000
	190	105.125	
	210	120.125	
	230	136.125	
	250		
	270		
	290		
	310		
	330		
	350		
	360		

SPENVIS

The next step in analysis was to utilize the European Space Agency's (ESA) Space Environment Information System (SPENVIS). SPENVIS is a web interface to models of space environment and its effects, including radiation belts and plasmas. Model packages of Earth, Mars and Jupiter are available. [37] In order to calculate the predicted radiation dosage for each trajectory, the time and position information produced via POST for all 16,416 flyby trajectories were run through SPENVIS. The following trapped particle models for Jupiter were utilized: The Galileo Interim Electron Environment (GIRE) and the Divine and Garrett Model (D&G83).

D&G83: Proton & Electron Model

The Divine and Garrett model is based on data collected by Pioneer, Voyager and Earth-based observations. Electrons are represented from the surface of the planet to the tail of the magnetosphere, while protons are represented from the surface to approximately 12 R_J. [38]

GIRE: Electron Model

The Galileo Interim Electron Environment model was developed using data from Galileo, Pioneer 10 and 11. Electrons are represented between ~8 and ~16 R_J. [34]

SHIELDOSE-2

SHIELDOSE-2 calculates space-shielding radiation doses. For given electron and proton particles encountered by a spacecraft, SHIELDOSE-2 determines the absorbed dose as a function of depth in aluminum shielding material. For the cases in this study, the chosen geometry was a solid sphere, with dose as a

function of sphere radius. The target material is silicon and the shielding material is aluminum. Radiation is from all directions. The geometry is illustrated in Figure 26. Results are listed as silicon dose in rads as a function of energy for fixed depths behind aluminum shielding material. [39]

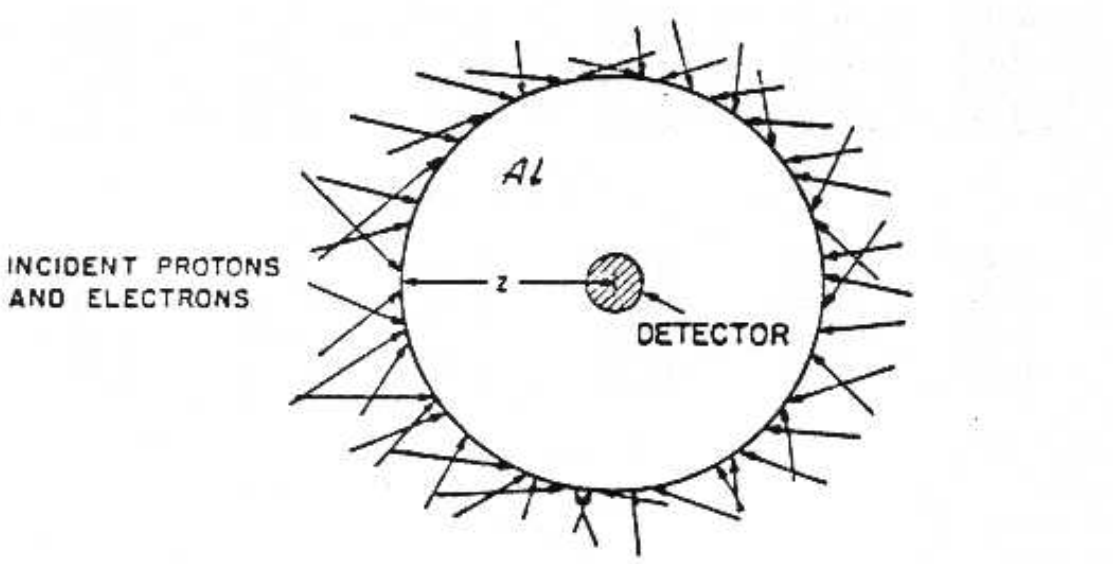

Figure 26. Geometry of absorbed dose as function of depth in aluminum shielding material. [39]

Development of Database and Estimation Tool

Once the desired trajectories were created in POST, they were run through a series of steps via SPENVIS. This ensured that the D&G83 and GIRE models were applied to the trajectories. Finally, the SHIELDOSE-2 analysis resulted in radiation dosages at a depth of 3 mm of aluminum. These values were saved for each trajectory. A database of radiation dosages for varying trajectories was established in Excel.

An estimation tool was created in order to estimate flyby radiation of trajectories that are not currently listed in the database. The tool uses multi-linear

interpolation and Excel's "look up table" function to predict the radiation. Accuracy of this estimation tool is discussed in the next chapter.

CHAPTER VI
RESULTS AND DISCUSSION

Database

The main product of this thesis is an Excel based database that can be used for the rapid approximation of spacecraft radiation during a Jupiter flyby. A screenshot of the finished product is shown in Figure 27. There are two options to approximate radiation dosage. First, the user may select their desired flyby parameters from a drop down list of pre-determined initial conditions. These values are listed in Table 3. The resulting predicted spacecraft radiation will be displayed instantly and will be as accurate as completing all the time intensive steps involved in the original process.

If the user has already selected their own flyby parameters and is interested in a rapid approximation, they may utilize the second option, which is the database estimation tool. This allows the user to input any parameters within the range of values listed in Table 3. The resulting predicted spacecraft radiation will be displayed instantly. The accuracy of these results are discussed in the next section.

Database Estimation Tool Accuracy

To determine the accuracy of the database estimation tool, a sample of 144 randomized Jupiter flyby trajectories was populated. Table 4 lists the flyby parameters for the comparison cases chosen to check the tool accuracy. The range of parameters was chosen in order to cover the full range of predicted radiation dosages. The dosages were populated via two methodologies: the original time intensive method and using the newly developed database estimation tool. The results of each process were then compared.

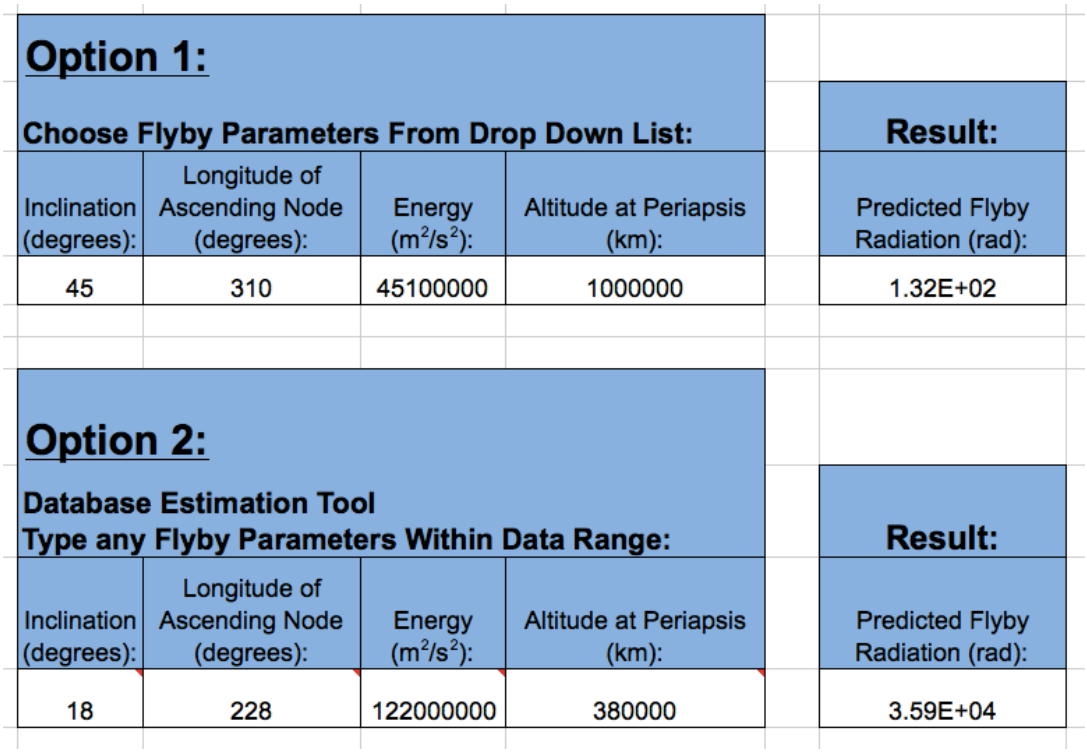

Option 1:

Choose Flyby Parameters From Drop Down List:

Inclination (degrees):	Longitude of Ascending Node (degrees):	Energy (m^2/s^2):	Altitude at Periapsis (km):
45	310	45100000	1000000

Result:

Predicted Flyby Radiation (rad):
1.32E+02

Option 2:

Database Estimation Tool
Type any Flyby Parameters Within Data Range:

Inclination (degrees):	Longitude of Ascending Node (degrees):	Energy (m^2/s^2):	Altitude at Periapsis (km):
18	228	122000000	380000

Result:

Predicted Flyby Radiation (rad):
3.59E+04

Figure 27. Screenshot of the database for rapid approximation of spacecraft radiation during a Jupiter flyby

Table 4. Flyby trajectory parameters for comparison cases

Inclination (degrees)	Longitude of Ascending Node (degrees)	Energy (km^2/s^2)	Altitude at Periapsis (km)
18 33 76	11 145 292	25.289 40.125 90.125 125.125	190000 500000 1220000 1750000

Figure 28 shows the direct correlation between the original method and the database estimation tool. The graph shows that the relationship is almost linear, with accuracy improving as dosage increases. Flyby trajectories with a dosage of less than 10 rad were considered but resulted in an increased error. Accuracy at such low doses is unreliable; therefore application of the tool is limited to doses above 10 rad.

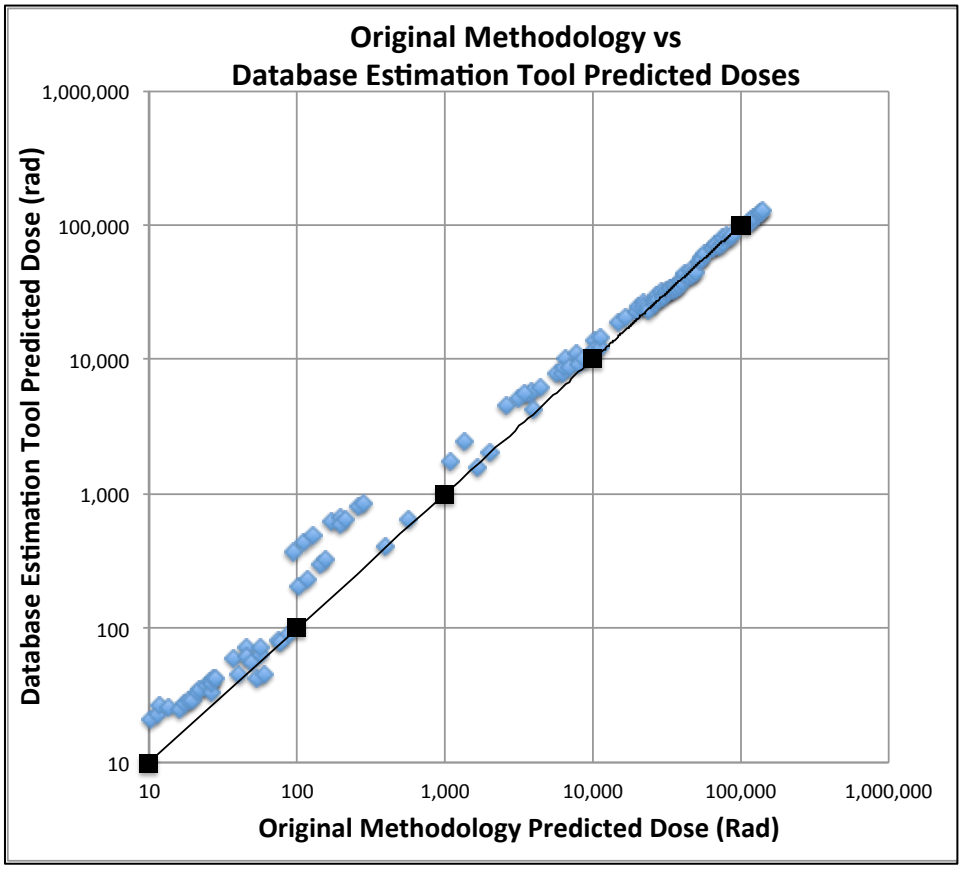

Figure 28. Original methodology vs Database Estimation Tool Predicted Doses

Figure 29 shows percent error for dosages greater than 1000 rad. The figure shows that percent error is generally lower for high dose cases. It also shows that the database estimation tool makes conservative estimates of the dosages for low dose cases (over prediction) and non-conservative estimates for high dose cases (under prediction).

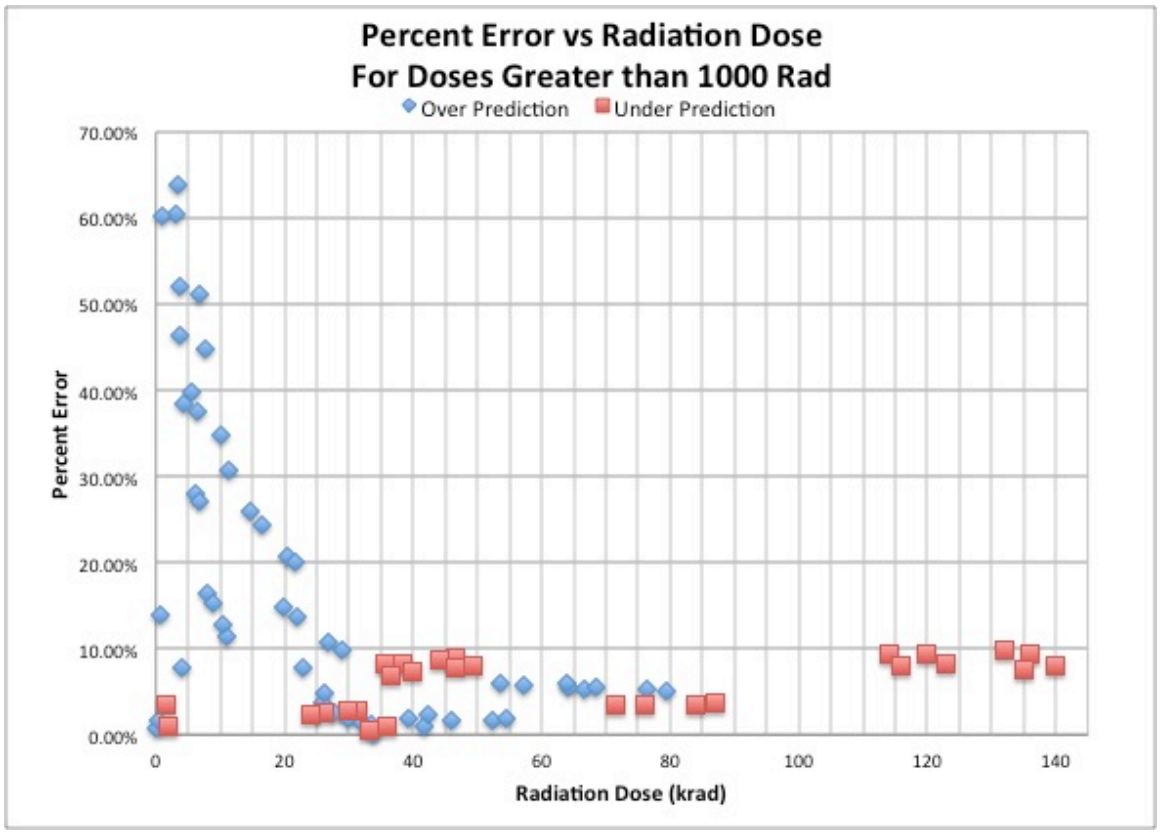

Figure 29. Percent Error vs Dose

Historical Radiation Doses

True radiation dose data for Jupiter flybys is limited. Dosage at a depth of 3 mm of aluminum has been published for both Pioneer 10 & 11 and Ulysses. Table 5 shows the observed dosages for Pioneer 10 and Ulysses versus the predicated doses using both methodologies. [40] [41] Dosage data for all other Jovian flybys is either missing or restricted to the public. Pioneer 11 had an altitude at periapsis of 42,840 km, which is considerably closer than the small periapsis altitude in the database of 100,000 km. This means approximating radiation for Pioneer 11 involves extrapolating rather than interpolating and cannot be predicted using the database estimation tool.

Table 5. Observed radiation dosages at 3 mm aluminum versus predicted radiation doses at 3 mm aluminum during Jupiter Flybys [40] [41]

Mission	Observed Radiation Dose	Predicted Radiation Dose (Original Methodology)	Predicted Radiation Dose (Database Estimation Tool)
Pioneer 10	280 krad	179.4 krad	152.9 krad
Pioneer 11	120 krad	68.72 krad	-----
Ulysses	60 krad	38.5 krad	36.6 krad

CHAPTER VII
CONCLUSIONS AND RECOMMENDATIONS

Effects of Each Jovian Flyby Parameter

During the development of the database, in order to keep the total number of cases reasonable, the influence of argument of periapsis on radiation dosages was not considered. I believed this to be justifiable since I expected the argument of periapsis to influence the dosage less strongly than some of the other trajectory characteristics such as periapsis altitude and inclination. In an attempt to determine if this was a reasonable assumption, the effect of argument of periapsis was examined for four different cases. For each trajectory, a quick look at the effects of argument of periapsis was examined. While holding inclination, longitude of the ascending node, energy, and altitude of periapsis constant, trajectories and corresponding dosages were populated for the full range of possibilities for argument of periapsis. The resulting predicted radiation dosages were populated using the original methodology – utilizing both POST and SPENVIS. Cases were strategically chosen in order to show a full range of predicted radiation dosage results. Case parameters are listed in Table 6. Figure 30 shows the results. One can see that dosages have peaks for trajectories with low periapsis altitudes. The database was developed using a constant argument of periapsis value of 295.5 degrees, which falls approximately in the middle range of dosage values for all cases. Future work should include an expansion of the database, which would include variations in argument of periapsis.

Table 6. Flyby cases with varying parameters

	Inclination (Degrees)	Longitude of Ascending Node (Degrees)	Energy (km^2/s^2)	Altitude at Periapsis (km)
Case 1*	45	310	451	100,000
Case 2	5	190	120.1	400,000
Case 3	20	30	28.1	100,000
Case 4	60	30	91.1	800,000

*Case 1 is similar to Pioneer 10

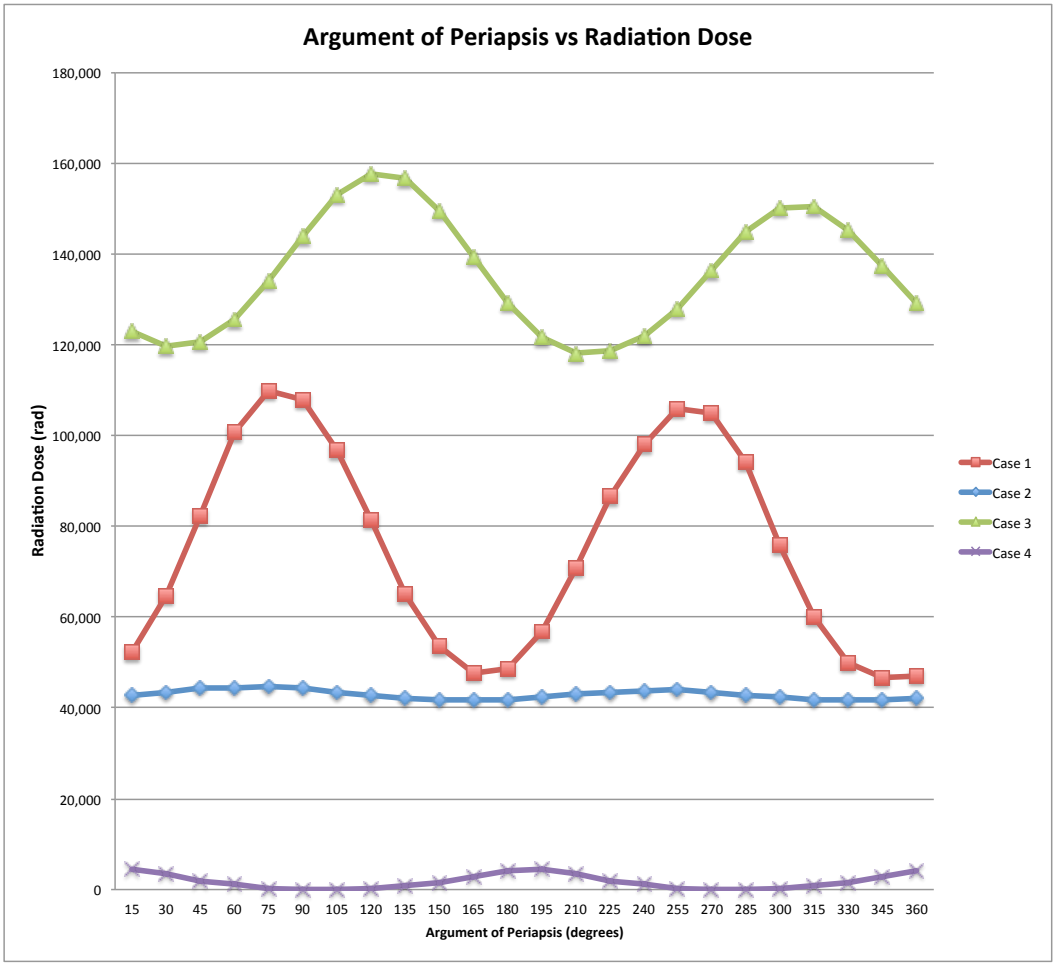

Figure 30. Argument of periapsis vs radiation dose

The range in predicted dosage for varying values for argument of periapsis is fairly small (maximum variation in dose of 120%) especially when compared to effects of varying other parameters. Figures 30-33 show the impact of varying each of the other parameters while holding all other values constant. The same four cases were examined for each parameter.

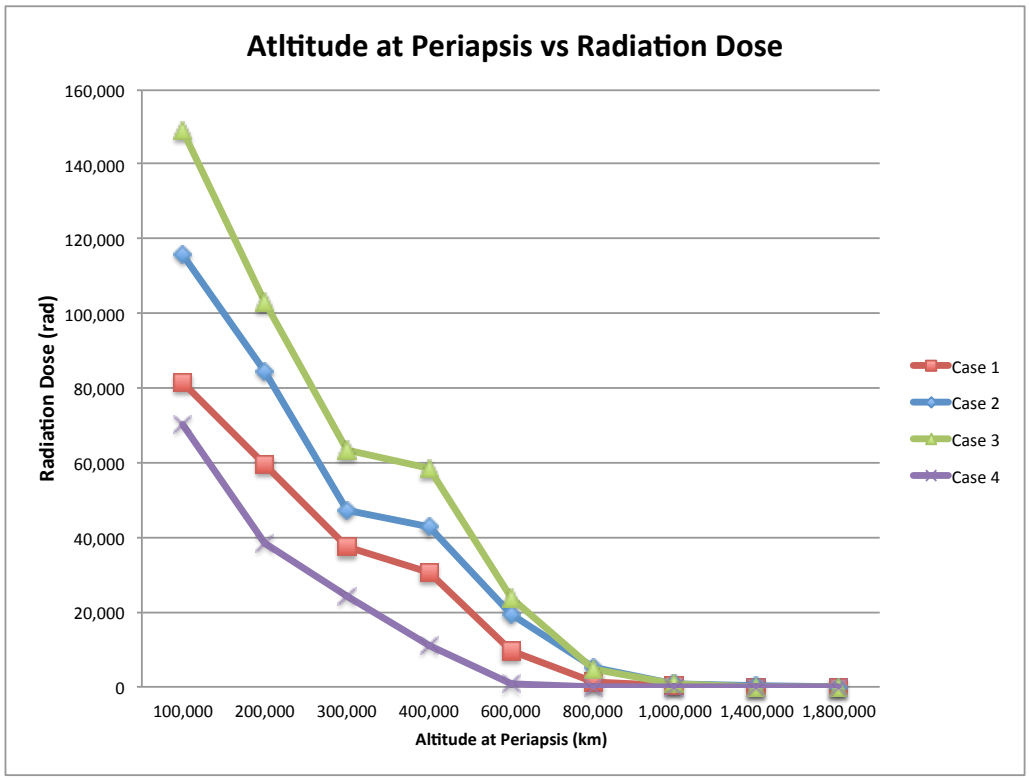

Figure 31. Altitude at periapsis vs radiation dose

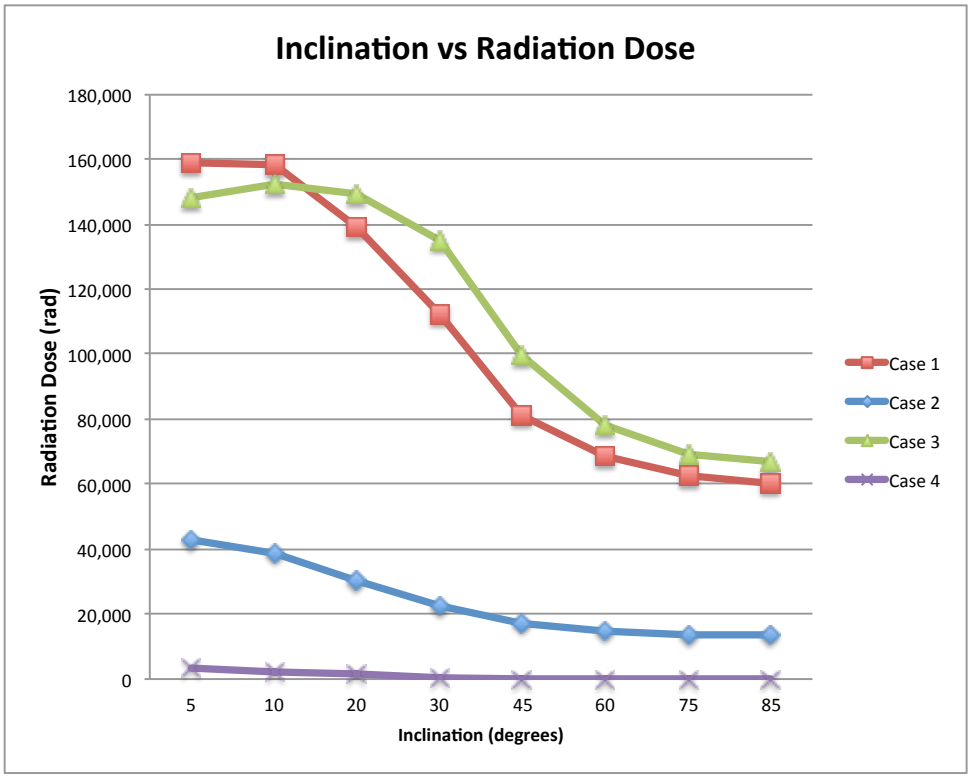

Figure 32. Inclination vs radiation dose

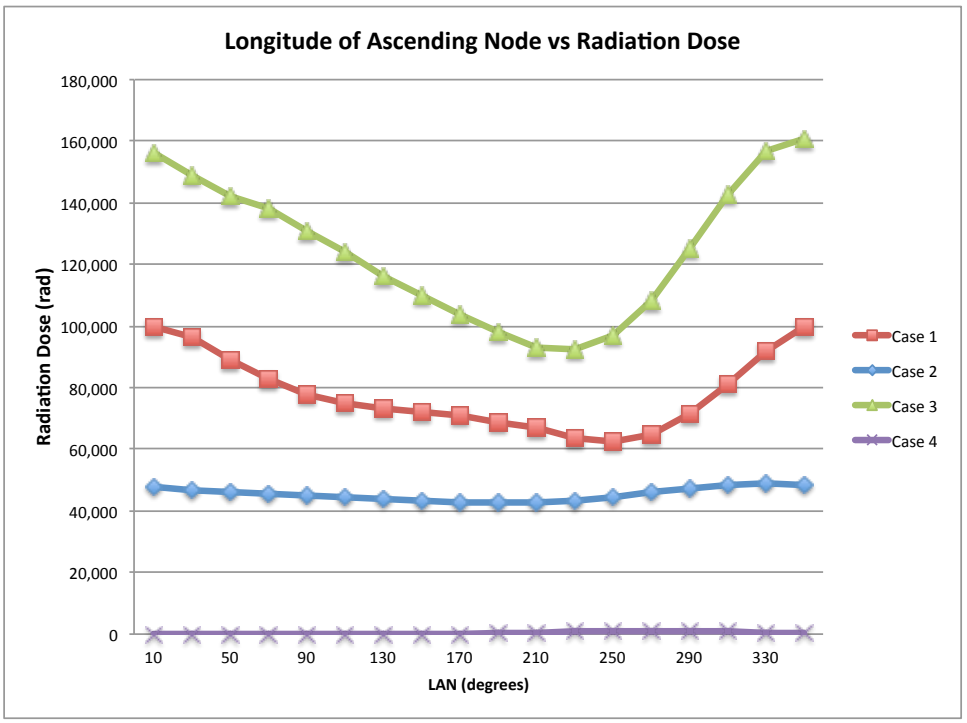

Figure 33. Longitude of the ascending node vs radiation dose

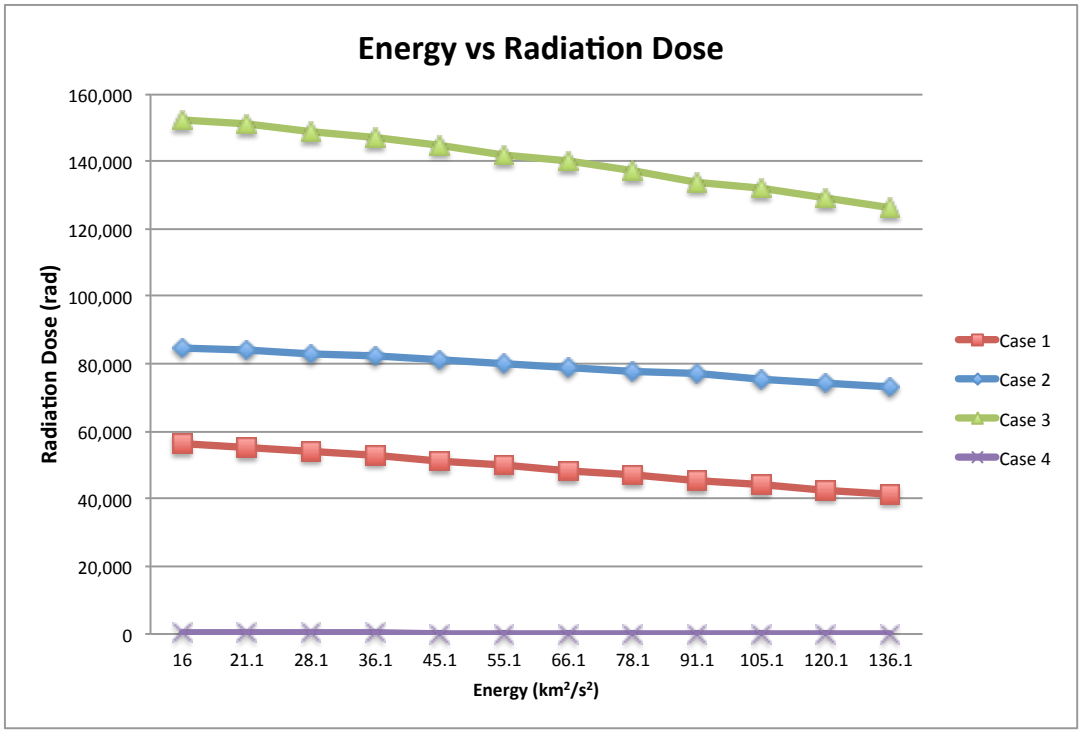

Figure 34. Energy vs radiation does

It is easy to see that altitude at periapsis has the greatest impact on radiation. Variations in dosages range up to a staggering 15,000%. Low periapsis altitudes result in higher radiation dosages. This correlation is intuitive since the Jovian trapped particle environment is most dense closest to the planet (see Figure 24). Inclination has the second greatest impact, with variations in dosages ranging up to 167%. Lower inclinations result in higher radiation dosages; this correlation can be easily explained since the particles in the Jovian longitudinal plane are somewhat squashed (see Figure 25). Longitude of the ascending node has a relatively small impact on radiation dosages, with variations ranging up to 68%. Finally, energy has the smallest impact on radiation dosages, with the greatest variation in dosage of 21%. Higher energies result in a slightly smaller radiation dose, since faster velocities mean there is less time that the spacecraft is exposed to Jupiter's radiation belts.

From these comparisons, one can see that the effects of argument of periapsis are approximately equal to inclination and longitude of the ascending node (at least for the cases considered). One can also conclude that argument of periapsis is perhaps more important than energy.

Future Work

Currently, there has been a discussion to incorporate the database estimation tool into the Mission Analysis Environment (MAnE) software. MAnE is a system of software used by space mission designers to support the analysis and optimization of multiple-leg, heliocentric missions which utilized conventional high-thrust propulsion. [42] Incorporating a Jovian flyby radiation component to the software would help streamline the decision making process for mission designers as they evaluate potential trajectories for deep space missions.

The finding that argument of periapsis may perhaps be more important than energy merits future work. It would be of value to add the fifth flyby parameter

to the database. Additionally, increasing the quantity and range of flyby parameters to the database would improve utility and accuracy.

It would also be advantageous to complete a more comprehensive error analysis, similar to the work shown in Figures 28 and 29 using more comparison cases. By looking a the 144 cases run so far, it seems like a multiplier might be used to make the predicted results better. A "correction factor" could be applied which would improve the results seen in Figure 28. Finally, we plan to put the database on the web for users to download free of charge to encourage its use.

LIST OF REFERENCES

1. Stern, A., et al., *The New Horizons Mission to Pluto and Flyby of Jupiter* 2008.
2. Cressler, J.D. and H.A. Mantooth, *Extreme Environment Electronics* 2013.
3. Flandro, G.A., *Fast Reconnaissance Missions to the Outer Solar System Utilizing Energy Derived from the Gravitational Field of Jupiter.* 1966.
4. Riley, C. and D. Campbell. *The Maths that Made Voyager Possible*. 2012 Accessed January 20, 2016]; Available from: http://www.bbc.com/news/science-environment-20033940.
5. *Professor Gary Flandro Named AIAA Fellow*. University of Tennessee Space Institute 2007 Retrieved January 20, 2016]; Available from: http://www.utsi.edu/news/2007/release12-17-07garyflandronamedaiaafellow.htm.
6. Flandro, G.A., *From Instrumented Comets to Grand Tours: On the History of Gravity Assist*, in *39th AIAA Aerospace Sciences Meeting and Exhibit*. 2001: Reno, NV.
7. McGranaghan, R., et al., *A Survey of Mission Opportunities to Trans-Neptunian Objects.* Journal of the British Interplanetary Society. **64**: p. 296-303.
8. McGranaghan, R., et al., *A Survey of Mission Opportunities to Trans-Neptunian Objects.* Advances in the Astronautical Sciences Series, 2012. **142**(CP11-615).
9. Allen, R., et al., *A Survey of Mission Opportunities to trans-Neptunian Objects – Part II, Orbital Capture*, in *Astrodynamics Specialist Conference*. 2012: Minneapolis, MN.
10. Kreitzman, J., Stewart, C., Cansler, E., Brisby, J., Green, M., and Lyne, J.E., *Mission Opportunities to trans-Neptunian Objects – Part III, Orbital Capture, Low Thrust Trajectories and Vehicle Radiation Environment during Jovian Fly-by*, in *Astrodynamics Specialist Conference*. 2013: Hilton Head, SC.
11. Gautamraj Baskaran, A.S.B., Justin D. Lewis, Kyle J. Malone, Harsh M. Ved and James Evans Lyne*, *A Survey of Mission Opportunities to Trans-Neptunian Objects – Part IV*, in *AIAA/AAS Astrodynamics Specialist Conference, SPACE Conferences and Exposition*. 2014: San Diego, CA.
12. Lyne, J.E., et al. *Potential Orbital Capture Missions to Trans-Neptunian Objects*. in *11th International Planetary Probe Workshop*. 2014. Pasadena, CA.
13. *Mission Analysis Environment (MAnE)*. Space Flight Solutions: Herdersonville, NC.
14. *Heliocentric Interplanetary Low-thrust Trajectory Optimization Program (HILTOP)*. Space Flight Solutions: Hendersonville, NC
15. Rirchard O. Fimmel, J.V.A., Eric Burgess, *Pioneer: First to Jupiter, Saturn and beyond*. 1980.
16. Allen, J.A.v., *Gravitational Assist in Celestial Mechanics-a Tutorial.* American Journal of Pysics 2003. **71**(5): p. 448-451.
17. NASA. *The Voyager Planetary Mission Fact Sheet*. [cited 2015 August 1]; Available from: http://voyager.jpl.nasa.gov/news/factsheet.html.
18. NASA. *Heliocentric View of Voyager Trajectories*. [cited 2015 August 1]; Available from: http://voyager.jpl.nasa.gov/science/heliocentric.html.

19. Cesarone, R.J., *A Gravity Assist Primer.* AIAA Student Journal, 1989. **27**: p. 16-22.
20. NASA. *Basics of Space Flight: Interplanetary Trajectories*. [cited 2015 August 1]; Available from: https://solarsystem.nasa.gov/basics/bsf4-1.php.
21. ESA. *Ulysses Factsheet*. [cited 2015 August 1]; Available from: http://www.esa.int/Our_Activities/Space_Science/Ulysses_factsheet.
22. Franc, T. *The Gravitational Assist*. in *WDS '11 Proceedings of Contributed Papers: Part III-Physics*. 2011. Prague: Matfyzpress.
23. Smith, E.J. and K.-P. Wenzel, *Introduction to the Ulysses Encounter with Jupiter.* Journal fo Geophsyical Research: Space Physics (1978-2012), 1993. **98**(A12): p. 21111-21127.
24. NASA. *Cassini Soltice Mission - Mission Overview*. [cited 2015 August 1]; Available from: http://saturn.jpl.nasa.gov/mission/introduction/.
25. Bolton, S.J., et al., *Cassini/Huygens flyby of the Jovian System.* Journal fo Geophsyical Research: Space Physics (1978-2012), 2004. **109**(A9).
26. NASA. *Cassini Mission Overview*. 2016 [cited 2016 1 February 2016]; Available from: http://saturn.jpl.nasa.gov/files/cassini_msn_overview.pdf.
27. Guo, Y. and R.W. Farquhar, *New Horizons Mission Design.* Space Science Reviews, 2009. **140**: p. 49-74.
28. Krupp, N., *New Suprises in the Largest Magnetosphere of Our Solar System.* Science, 2007. **318**: p. 216.
29. Blattnig;, R.N.F.B.W.A.S., *A Deterministic Electron, Photon, Proton and Heavy Ion Radiation Transport Suite for the Study of the Jovian System.* Aerospace Conference, 2011 IEEE, 2011.
30. Kivelson, K.K.K.M.G., *The Configuration of Jupiter's Magnetosphere.* 2004.
31. Astronomy, U.o.O. *Jupiter: Giant of the Solar System*. 1 February 2016]; Available from: http://pages.uoregon.edu/jimbrau/astr121/Notes/Chapter11.html.
32. McComas, D.J., *Diverse Plasma Populations and Structures in Jupiter's Magnetotail.* SCIENCE, 2007. **318**(217).
33. Thorheim, O. *Electronics in Space*. Interrup Inside 2016 1 March 2016; Available from: http://www.datarespons.com/electronics-in-space/.
34. ESA. *The Trapped Particle Radiation Environment of Jupiter*. 1 November 2015]; Available from: https://www.spenvis.oma.be/help/background/planetary/traprad_jup.html.
35. Garrett, H.B., et al., *Galileo Interim Radiation Electron Model,*. JPL 03-006, 2003.
36. Brauer, G.L., D.E. Cornick, and R. Stevenson, *Capabilities and Applications of the Program to Optimize Simulated Trajectories (POST),*. 1977: NASA.
37. ESA. *SPENVIS The Space Environment Information System*. 1 November 2015]; Available from: https://www.spenvis.oma.be/.
38. Divine N. and Garrett H. B., C.p.d.i.J.s.m., J. Geophys. Res., 88, 6889-6903, 1983.
39. Seltzer, S.M., SHIELDOSE, A Computer Code for Space-Shielding Radiation Dose Calculations, National Bureau of Standards, NBS

Technical Note 1116, U.S. Government Printing Office, Washington, D.C., 1980.
40. Miller, M.W., G.E. Kaufman, and H.D. Maillie, *Pioneer 10 and 11 Jovian Encounters: Radiation Dose and Biological Lethality*. Life Sciences and Space Research, 1976. **14**: p. 195-199.
41. Podzolko, M.V., et al. *Charged particle fluxes in Earth-Jupiter-Europa spacecraft's trajectory*. in *European Planetary Science Congress* 2008. Munster, Germnay.
42. Horsewood, J. *Space Flight Solutions*. MAnE General Overview 2016; Available from: http://spaceflightsolutions.com/products/mane.asp.

VITA

Sarah Gilbert Stewart was born in Cleveland, TN to Dan and Betsy Gilbert. She is the oldest of three children; her siblings are Leah and Adam. She attended the Georgia Institute of Technology and received her Bachelor of Science degree in Aerospace Engineering with High Honors in December 2009. Upon graduation, she commissioned into the United States Air Force. Sarah served as an active duty officer for nearly four years, working as an operations engineer for military spacecraft. After leaving the Air Force, she accepted a graduate teaching assistantship at the University of Tennessee in the College of Engineering. Sarah is married to Brian Stewart and together they have one son, Levi Daniel Stewart. Sarah is graduating with a Master of Science degree in Aerospace Engineering.